Construction of 1961-90 High-Resolution monthly Temperature climatologies for Northern Italy

Technical Report

Jonathan Spinoni [1], Michele Brunetti [2], Gianluca Lentini [1], Maurizio Maugeri [1], Teresa Nanni [2]

1 University of Milan, Institute of General Applied Physics, Milan, Italy.
2 Institute of Atmospheric Sciences and Climate, Italian National Research Council (ISAC-CNR), Bologna, Italy.
mail to: jonathan.spinoni@unimi.it

1. Introduction

This technical report presents the activities performed by the University of Milan and ISAC-CNR Research Group in the frame of the ECSN/HRT GAR project. Such activities addressed the construction of 1961-90 High-Resolution monthly Temperature (HRT) climatologies for Northern Italy. These climatologies were obtained by means of a geographical model aiming at capturing the dependence of temperatures on a number of geographical and morphological features.

The general goal was to estimate monthly temperature climatic normals (clinos) on a regular grid (1 km^2 resolution) covering all Northern Italy and part of Central Italy. This estimation was checked by means of a 664 station network in order to keep the mean absolute error (MAE) and the root mean squared error (RMSE) below the optimal threshold of 1 °C.

2. Data

The data used for the construction of the monthly HRT climatologies are monthly climatic normals (1961-90) of 664 stations within a 576,000 km^2 area encompassed by 6-14 °E and 42.5-47.5 °N longitude and latitude limits. The spatial distribution of such stations (fig.1) is sufficiently homogeneous, even though two regions (French Alps, the Marche) are poorly covered. The average station density is 1 station each 870 km^2 (1 station each approximately 600 km^2 without considering the seas). The stations are evenly located in plain, hill and mountain areas (fig. 2).

Beyond the station data, the 1 km^2 GTOPO30 digital elevation model (DEM) was used. The Italian data were provided by: University of Turin, University of Padova, University of Pavia, SIMN (the former Italian Hydrographic Service), Autonomous Province of Bozen, SMI (Italian Meteorological Society), AMI (Italian Military Aviation), UCEA (Central Office of Economical Agriculture).

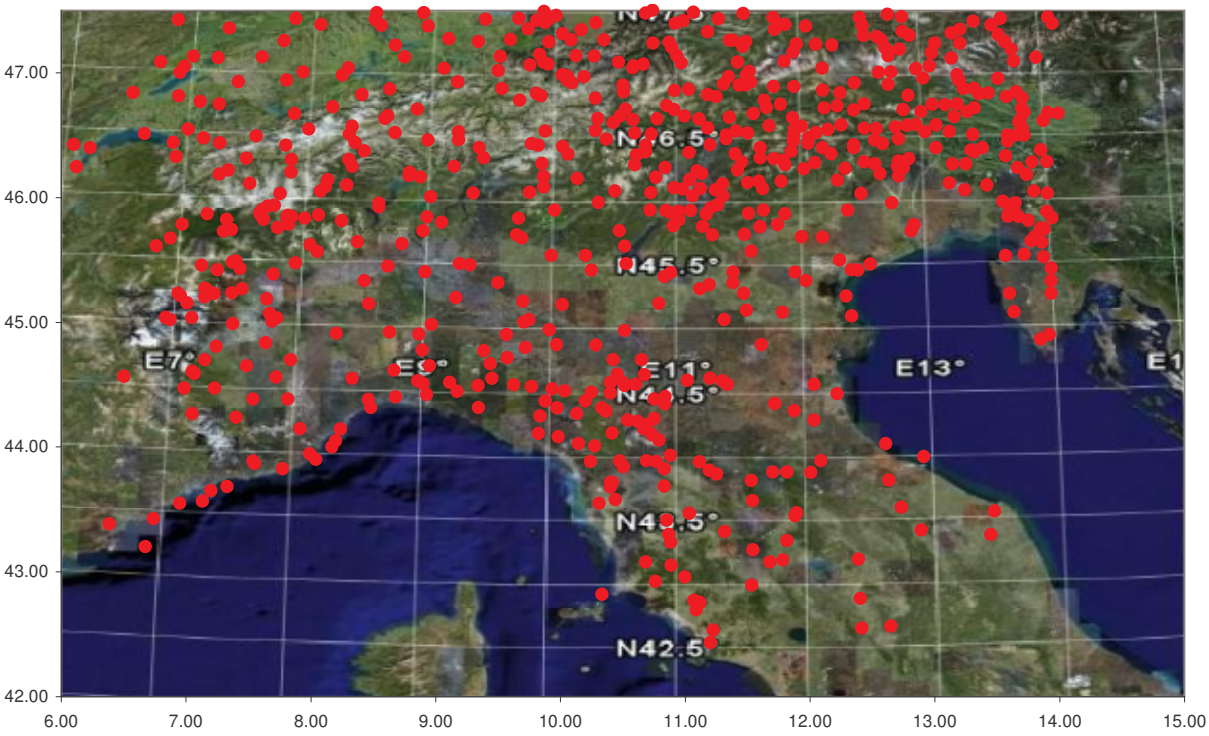

Fig. 1 : Spatial distribution of the stations used for the construction of the HRT climatology.

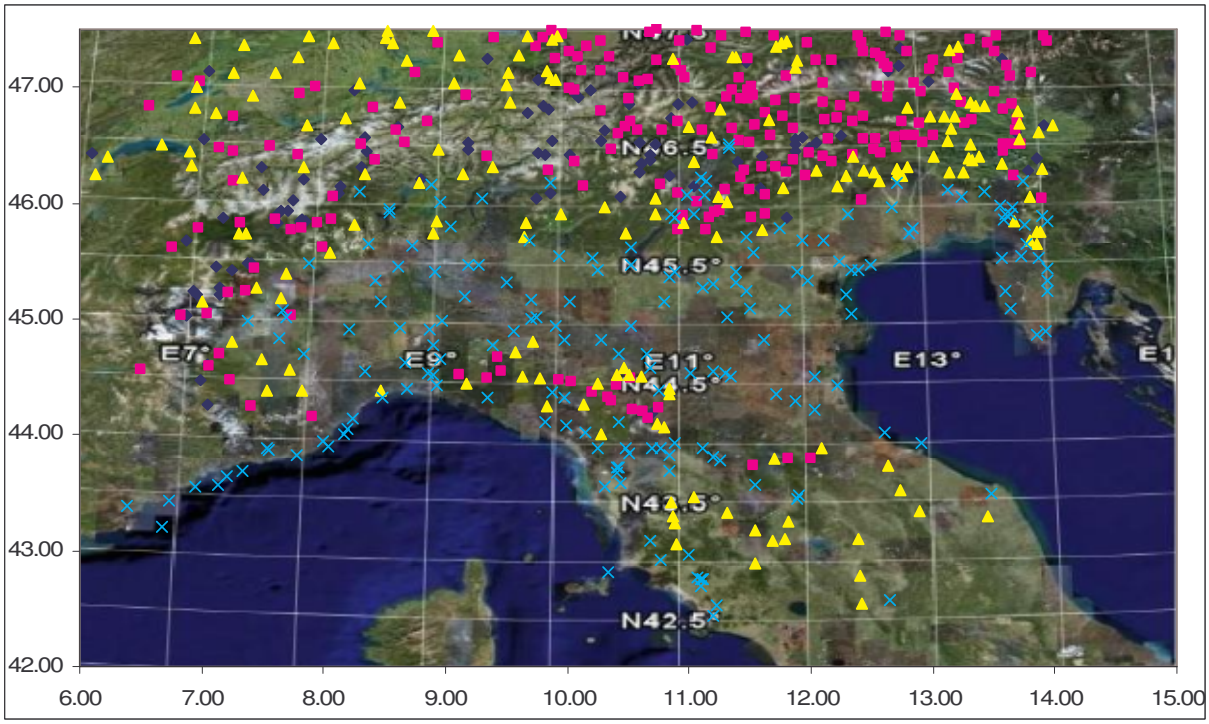

Fig. 2 : Elevation distribution of the stations in our data-set: light blue crosses indicate plain stations, yellow triangles represent hill stations, scarlet squares are referred to mountain stations.

3. The geographical model (Part I: leading variables)

3.1 Temperature versus Elevation

The first variable considered in the geographical model was elevation. The obvious physical reason for this is the progressive vertical cooling of the air due to the fact that the atmosphere is primarily warmed by the heat emitted from the Earth's surface. Such an effect is well known from literature, even though in large part of the area under examination important thermal inversions do occur, especially in winter. Such thermal inversions significantly reduce the correlation among temperature and elevation, causing the common variance (R^2) to drop from about 0.9 in late spring and summer to approximately 0.65 in late autumn and winter months.

The first attempt to capture the elevation dependence of temperature consisted in a two-layer model obtained by applying linear regression to two subsets of stations: the stations from 0 m to 1500 m and the stations from 1500m to 4000m. Actually, such an attempt, though reasonable for an area with complex orography, did not work properly as for several months, a discontinuity of about 2 °C was found. So it was decided to simply perform a linear regression over the whole database, even though in order to reduce the error, coast stations (less than 50 km from the Ligurian, Tyrrhenian or Adriatic Sea), lake stations and urban stations were not considered.

This linear regression was performed on a monthly basis: it allowed to obtain the following relation:

$$T_{stations} = aH_{stations} + b$$

where *a* is the vertical lapse rate and *b* the temperature at 0 m.
As expected, the highest (in absolute value) vertical lapse rates were found for summer months (e.g. July: -0.68°C / 100 m, see fig.4), whereas the lowest ones were found for winter (e.g. January -0.43°C / 100 m, see fig.3).

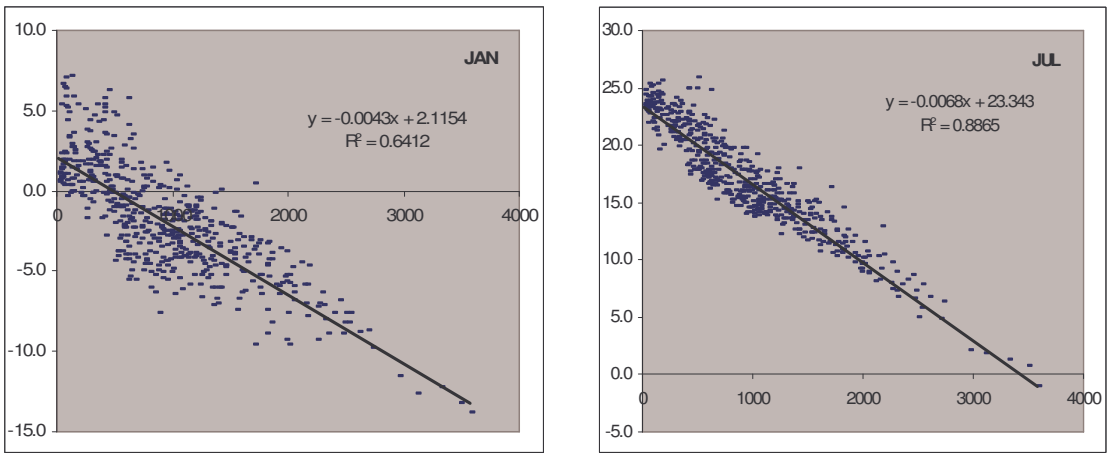

Fig. 3-4 : Temperature vs. elevation for January and July

Once the temperature dependence on elevation was obtained on the basis of the station data, it was assumed that the same dependence could be extended to the whole area represented by the 1 km^2 grid.

Such a procedure can be summarized in the following two steps:

1.) We got a,b *by a linear regression* $T_{stations}$ *vs* $H_{stations}$

2.) Using the same coefficients a,b ⇨ *we calculated* $T'_{model} = aH_{model} + b$ *for each grid cell of the considered area.*

where H_{model} is the elevation of the grid cell from GTOPO30 digital elevation model (it is the average elevation of the cell, not the elevation of the grid cell's centre).

The result of this procedure is an estimation of the normal temperature value of each grid cell (1 km^2 resolution).

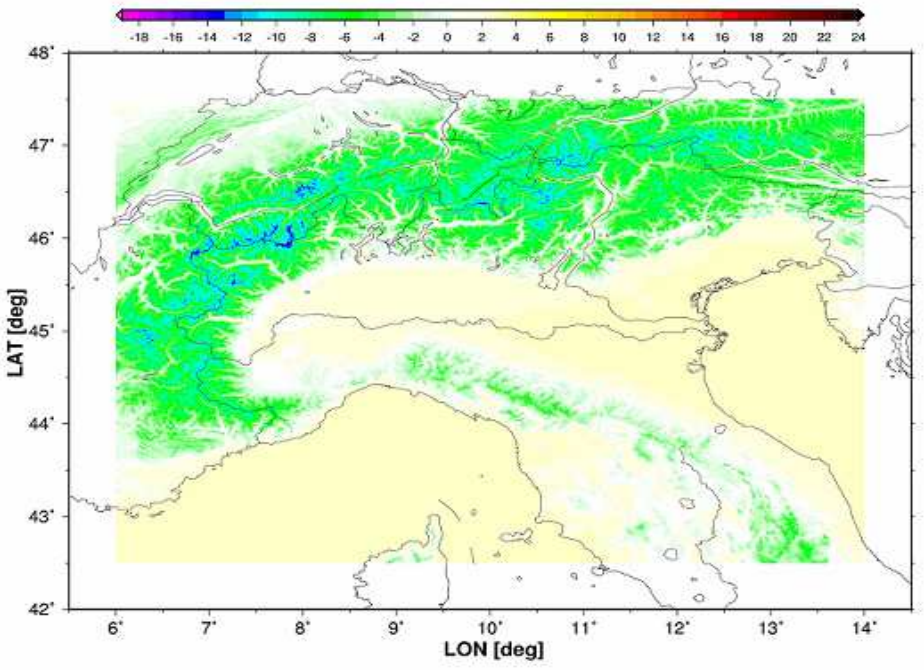

Fig. 5 : Temperature map of January obtained with a model considering only the temperature dependence on elevation

The next step was the comparison between the modelled normal temperatures and the observed values. Such a comparison was performed by studying the residuals, that are the differences between the observed temperature and the modelled normal values of the stations.
Such a procedure can be summarized by the following steps:

3.) Using a, b , $H_{stations}$ ⇨ *we calculated back* $T_{station\,\mathrm{mod}elled} = aH_{station} + b$ *for each station*

4.) From $T_{station}$, $T_{station\,\mathrm{mod}elled}$ ⇨ *we calculated the residual* $R_{station} = T_{station} - T_{station\,\mathrm{mod}elled}$ *for each station.*

If the residual (*R*) is positive the model assigns to the station a temperature value that is colder than the real measured value, vice versa, if the R value is negative the model assigns to the station a temperature value that is warmer than the real measured value.
The study of the residuals allows both to check the overall accuracy of the model and to represent the geographical pattern of the residuals. The study of such residuals is a key issue in the selection of further variables to be considered in order to improve the model's ability to capture the geographical complexity of the territory.
The overall accuracy of the model, including only the temperature dependence on elevation, was evaluated for each month of the year by means of the following statistical parameters: mean error (ME), mean absolute error (MAE) and root mean squared error (RMSE), see fig.6.

	Jan	Feb	Mar	Apr	May	Jun	Jul	Aug	Sep	Oct	Nov	Dec	Average
ME	0.42	0.26	0.15	0.04	-0.07	-0.11	0.04	0.07	0.17	0.22	0.38	0.46	**0.17**
MAE	1.80	1.43	1.08	0.95	0.92	1.09	1.24	1.24	1.12	1.23	1.45	1.84	**1.28**
RMSE	2.35	1.88	1.36	1.16	1.11	1.32	1.54	1.54	1.41	1.58	1.89	2.37	**1.63**

Fig. 6 : Accuracy of the model including only the dependence of temperature on elevation.

Such results highlight that, by considering only elevation, the geographic model would still be very far from the optimal threshold of 1.0°C for MAE and RMSE. In particular, the high RMSE values suggest that there are several stations with rather high absolute residuals, because RMSE is enhanced by the biggest errors.

The spatial behaviour of the residuals was studied by plotting the distribution of the residuals, see e.g. fig. 7 for January.

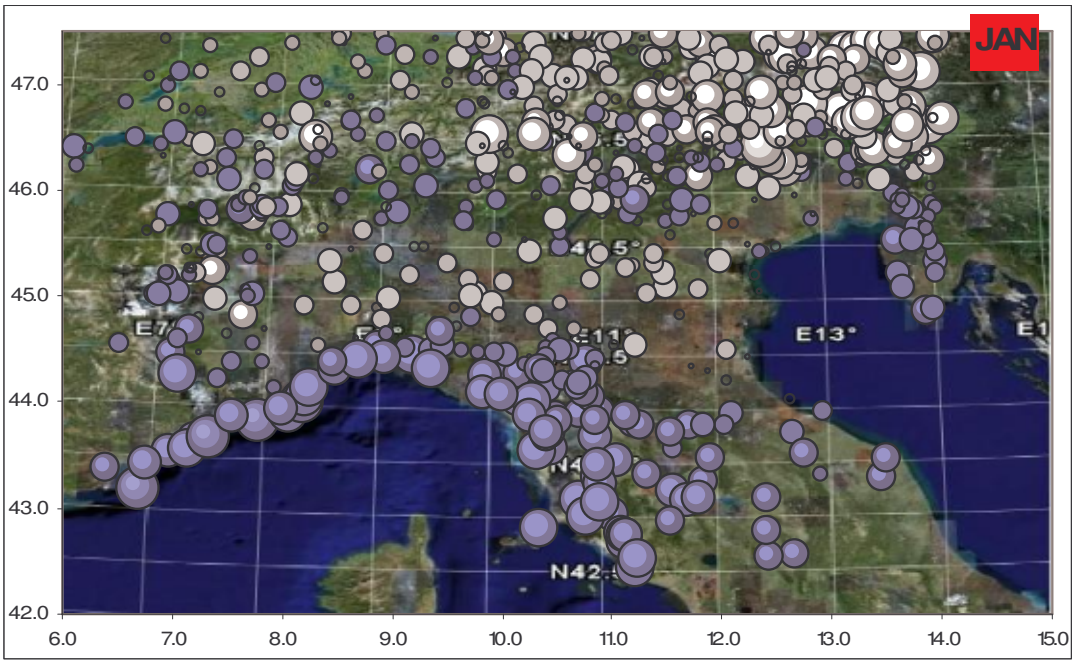

Fig. 7 : Spatial distribution of the residuals of the model including only the temperature dependence on elevation for January: blue bubbles represent positive residuals, white bubbles are related to negative residuals. The size of a bubble is proportional to the size of the residual.

Such plots highlight that a model developed only considering temperature versus elevation is not satisfactory (fig.6): in fact the residuals show a non-negligible latitude effect, a Po Plain cold winter pool in the lowlands, a remarkable sea effect, a slight longitude effect, a very small urban heat island effect, an inversion effect in the Alpine and Apennine valleys and a different sea effect between Ligurian and Tyrrhenian Seas and Adriatic Sea.

3.2 Temperature versus Latitude

The second variable considered in the geographical model was latitude. The obvious physical reason is the progressive decrease of temperature from the Equator to the Poles (approximately -0.8/-1.4 °C/ degree at mid-latitudes) due to the different radiative budget at the Equator and the Poles (Pinna,1977).

The approach was similar to the one assumed while considering temperature versus elevation, but from this second step on the residuals obtained from the previous step were used in the linear regressions.

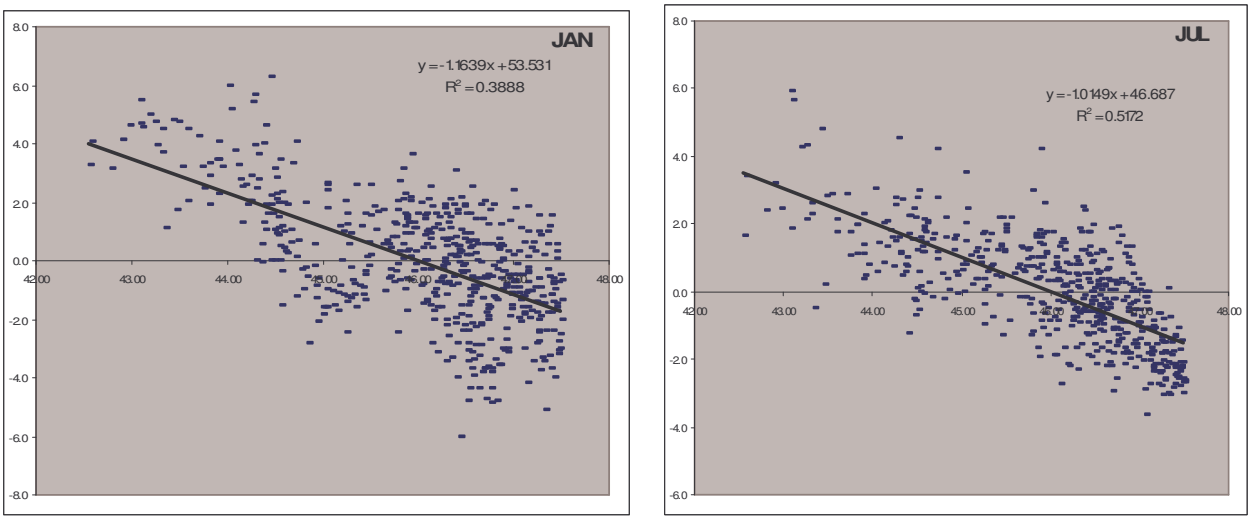

Fig. 8-9 : Temperature residuals (after taking into account the temperature dependence on elevation) vs. latitude for January and July

Such a procedure can be summarized by the following two steps:

1.) From $R'_{stations}$ *at 1st step* ⇨ *we found c, d from regression* $R'_{stations} = c(Lat)_{stations} + d$

2.) Using the same coefficients c, d ⇨ *we calculated* $R''_{model} = c(Lat)_{model} + d$

where *c* represents the temperature decrease for each latitude degree and *Lat*$_{model}$ is the latitude of the grid cell from GTOPO30 digital elevation model (that is latitude of the grid cell's centre). The latitude dependence of temperature ranges from -0.77 °C / °Lat in March to -1.35 °C / °Lat in January, whereas the average value over the year is -0.92 °C / °Lat . Such a decrease gives a difference of approximately 4 °C between Rome and Milan in winter and, for example, in March a grid cell at 43 °N is, only considering latitude, approximately 5.4 °C warmer than a grid cell at 47 °N.
The common variance coefficient of the linear regression between temperature and latitude ranges from 0.28 (May) to 0.56 (October).

The next step was the comparison between the modelled normal temperatures and the observed values. As discussed for elevation, such comparison was performed by studying the residuals.

In other words, the estimated temperature of each station according to the model, including the effects of elevation and latitude, was first obtained and, secondly, the difference between the observed and modelled values for each station was calculated.

Such a procedure can be summarized by the following steps:

3.) Using c, d $,(Lat)_{stations}$ ⇨ *we calculated back* $R''_{station\,\mathrm{mod}elled} = c(Lat)_{station} + d$ *for each station*

4.)From $R'_{station}$, $R''_{station\ \mathrm{mod}\ elled}$ ⇨ *we calculated the new residual* $R''_{station} = R'_{station} - R''_{station\ \mathrm{mod}\ elled}$ *for each station*

5.) We used $T''_{\mathrm{mod}el} = T'_{\mathrm{mod}el} + R''_{\mathrm{mod}el}$ *for each grid cell of the considered area.*

As for the elevation, also in this case, the overall accuracy of the model was evaluated by means of the following statistical parameters: ME, MAE and RMSE, see fig. 10.

	Jan	Feb	Mar	Apr	May	Jun	Jul	Aug	Sep	Oct	Nov	Dec	Average
ME	0.21	0.14	-0.02	-0.07	-0.12	-0.14	-0.15	-0.08	0.04	0.10	0.16	0.20	***0.02***
MAE	1.36	1.01	0.77	0.75	0.75	0.85	0.91	0.84	0.76	0.83	1.00	1.35	***0.93***
RMSE	1.68	1.28	0.99	0.94	0.96	1.08	1.16	1.05	0.95	1.07	1.26	1.67	***1.17***

Fig. 10 : Accuracy of the model including only the dependence of temperature on elevation and on latitude

Such results highlight that, by considering elevation and latitude, the geographical model would still be above the optimal threshold of 1.0°C for RMSE, but the MAE is below this threshold. Both MAE and RMSE are considerably smaller after this second step: MAE is smaller than 1.0°C and RMSE is 1.17°C, but in 4 months out of 12 it is already smaller than 1.0°C.

Also in this case, the spatial behaviour of the residuals was studied by plotting the distribution of the residuals, see e.g. fig. 11 for January.

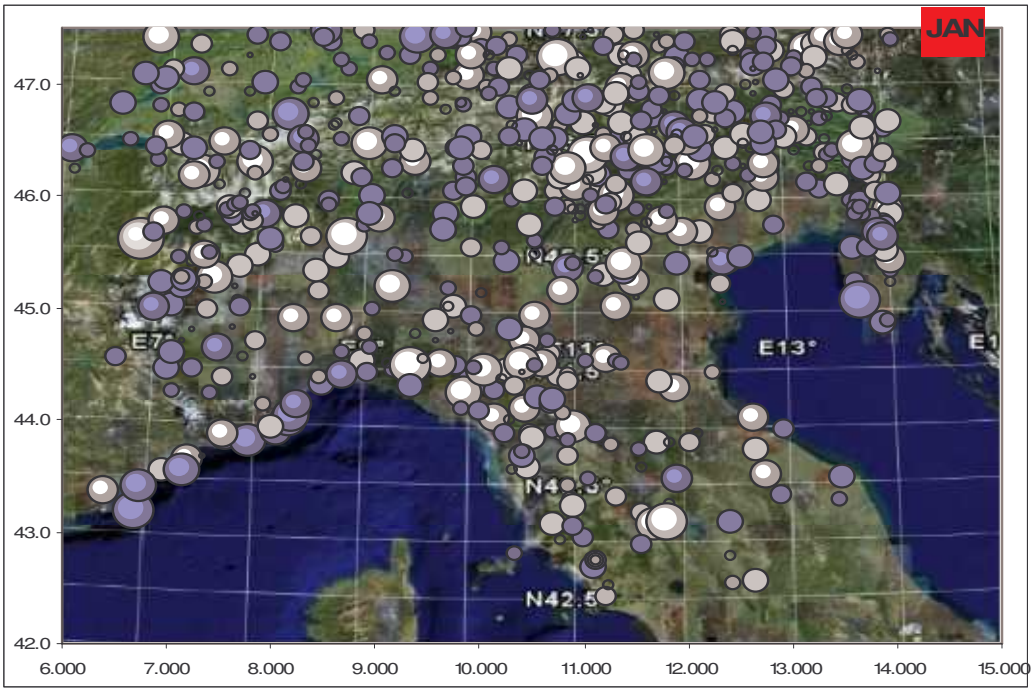

Fig. 11 : Spatial distribution of the residuals after considering elevation and latitude for January: blue bubbles represent positive residuals, white bubbles are related to negative residuals. The size of a bubble is proportional to the value of the residual.

Such plots highlight that a model developed only considering temperature versus elevation and latitude is not satisfactory: in fact, e.g., from the residuals map of July (fig. 11) the sea effect (a cooling effect) is evident and the same can be said for the lake effect.

3.3 Temperature versus Longitude

The third variable considered in the geographical model was longitude. The inclusion of longitude among the variables that can influence temperature normals is due to the fact that the area under examination, especially the Po Plain, tends to show an Eastward increasing continentality.

The data display that the longitude effect is completely negligible in summer months, but it is not negligible in winter months (fig. 12-13).

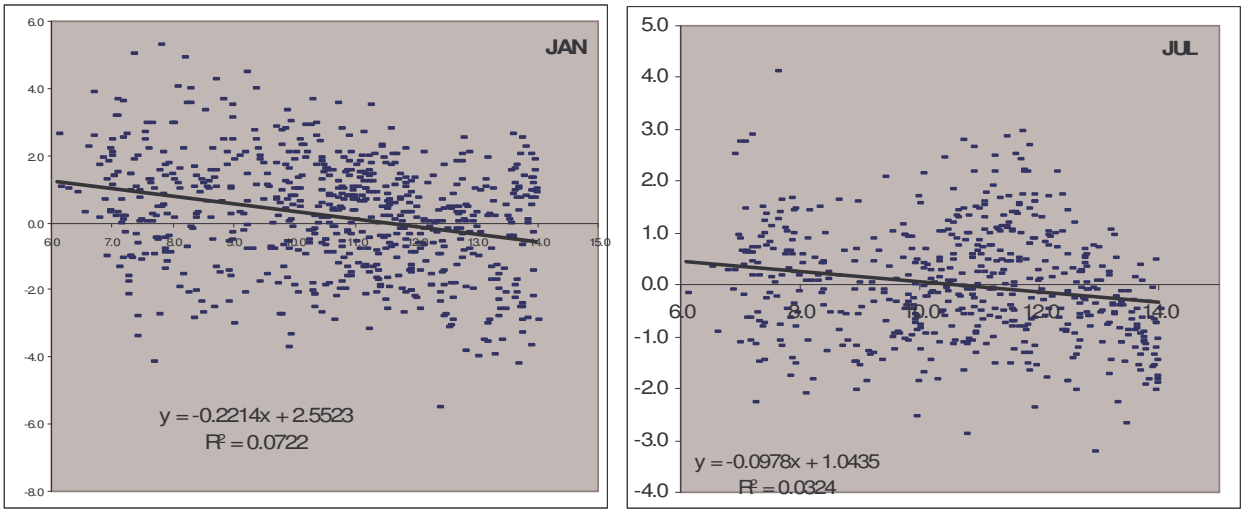

Fig. 12-13 : Temperature residuals after taking into account the temperature dependence on elevation and longitude versus longitude for January and July.

The approach adopted for longitude was the same used for temperature versus elevation or versus latitude.

Such a procedure can be summarized by the following two steps:

1.) From $R''_{stations}$ *at 2nd step* ⇨ *we found e, f from regression* $R''_{stations} = e(Lon)_{stations} + f$

2.) Using the same coefficients e, f ⇨ *we calculated* $R'''_{\mathrm{mod}\,el} = e(Lon)_{\mathrm{mod}\,el} + f$

where *e* represents the temperature variation for each longitude degree, *Lon*$_{model}$ is the longitude of the grid cell from GTOPO30 digital elevation model (that is longitude of the grid cell's centre). For example, it was found a longitude effect of 0.22 °C / °Lon in January (see fig. 12) and of -0.098 °C / °Lon for July (see fig. 13),

The common variance coefficient varies from 0.0002 (August) to 0.0831 (December), that is, the variance explained by this linear regression never exceeds 8.3%.

The next step was the comparison between the modelled normal temperatures and the observed values. As in the previous steps, such a comparison was performed by studying the residuals.

In other words, the estimated temperature of each station according to the model including the elevation, the latitude and the longitude effects was calculated first and, secondly, the difference between the observed and modelled values for each station was calculated.

Such a procedure can be summarized by the following steps:

3.) Using $e, f, (Lon)_{stations}$ ⇨ *we calculated back* $R'''_{station\,modelled} = e(Lon)_{station} + f$ *for each station*

4.)From $R''_{station}$ $R'''_{station\,modelled}$ ⇨ *we calculated the new residual* $R'''_{station} = R''_{station} - R'''_{station\,modelled}$ *for each station*

5.) We used $T'''_{model} = T''_{model} + R'''_{model}$ *for each grid cell of the considered area.*

Once again, the overall accuracy of the model was evaluated by means of the following statistical parameters: ME, MAE and RMSE, see fig. 14.

	Jan	Feb	Mar	Apr	May	Jun	Jul	Aug	Sep	Oct	Nov	Dec	Average
ME	0.19	0.11	-0.01	-0.10	-0.13	-0.15	-0.15	-0.09	0.01	0.12	0.15	0.19	***0.01***
MAE	1.33	0.98	0.75	0.74	0.75	0.85	0.90	0.83	0.75	0.83	1.00	1.32	***0.92***
RMSE	1.62	1.22	0.95	0.94	0.96	1.08	1.15	1.05	0.95	1.07	1.25	1.62	***1.15***

Fig. 14 : Accuracy of the model including the dependence of temperature on elevation, latitude and longitude.

The statistical parameters show a small improvement after this third step (for MAE and RMSE) but the intrinsic bias is still present in all months. The only important enhancements are noticeable in January and December.

By considering only the three main geographical parameters (elevation, longitude, latitude) the model satisfies the MAE threshold of 1.0 °C, but not the RMSE one. Anyway, at this point, the general features of the statistical errors were quite satisfactory, this is the reason why many spatialization climate models in literature consider just three parameters: elevation, latitude and longitude. The main problem was the unsatisfactory spatial pattern obtained: some important geographical effects, such as the sea effect, were not taken into account. So, it was necessary to evaluate secondary geographical and orographical effects.

4. Statistical Analysis (Part II : secondary effects)

4.1 Facet / slope exposure and summit / valley effects

The residuals obtained after taking into account the three leading geographical effects discussed in chapter 3 were further subjected to analyses aiming at identifying more significant relations between temperature and as many geographical and morphological features as possible. Such analyses were performed by plotting the spatial distribution of the residuals and by comparing the average residuals of particular subsets of stations.
The first morphological effect that was taken into account was the summit or the valley location. A summit station was expected to measure warmer temperature (thus, positive residuals) than a valley station. The reason is that a mountain top location receives more hours of direct solar radiation than a valley station and it is not subjected to the cooling effect due to negative radiative balance at the surface, which produces thermal inversions during the night.

In order to investigate such an effect, a summit station was defined as a station belonging to a grid cell whose elevation is higher than the eight surrounding cells (among these, only stations located at elevations higher than 400 m were considered, and stations on the mountain or hill slopes were rejected), while on the other side, a valley station was defined as a station belonging to a grid cell whose elevation is lower than the eight surrounding cells (among these, only stations located in mountain areas were considered as valley stations, while stations on the Po Plain, for example, were rejected). Stations located on mountain passes were considered as valley stations for they are climatologically similar to valley stations for temperature. According to these definitions, approximately 75 summit stations and 105 valley stations were identified.

The monthly averages of summit and valley station residuals are shown in fig. 14. The results confirm the different thermometric behaviour of summit and valley locations especially in winter, when the difference between summit and valley residuals can get to about 2.5°C.

	Jan	Feb	Mar	Apr	May	Jun	Jul	Aug	Sep	Oct	Nov	Dec
Summit	1.34	0.86	0.43	0.18	0.06	0.04	0.18	0.24	0.37	0.65	0.93	1.39
Valley	-0.95	-0.53	-0.16	0.12	0.24	0.31	0.33	0.18	-0.05	-0.39	-0.59	-1.01

Fig. 14 : Average residuals of summit and valley stations

The second morphological effect considered was the geographical slope exposure (hereinafter "facet"). The stations' facets were estimated by associating the grid cells facet values provided by GTOPO30 digital elevation model to any pertaining station. Such grid cell facets were simply calculated as the direction of the gradient of the function

$$Z = z\,(x\,,\,y)$$

where z is the elevation and x and y are the coordinates defined according to, respectively, Eastward and Northward axes. (See fig. 15)

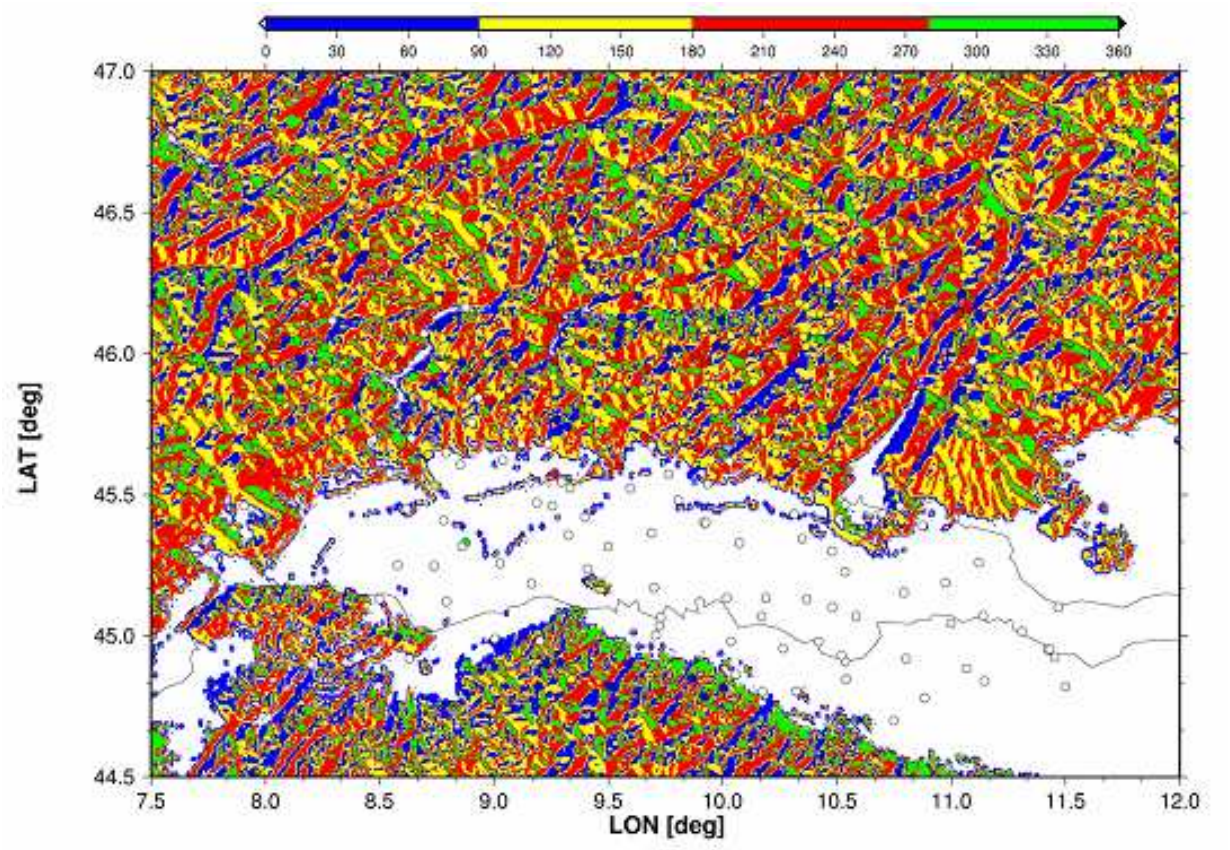

Fig. 15 : Facet exposure map: degrees are calculated from North (0°) to South (180°) counter-clockwise, that is W (90°) and E (270°). Of course GTOPO arbitrarily assigns a spurious value to plain grid cells.

Naturally, positive residuals were expected for South-facing stations and negative residuals for North-facing stations. The analysis of the residuals, that was performed after excluding summit and valley stations and stations belonging to cells whose slope is lower than 0.05, did not produce remarkable results for North-facing stations (i.e. stations whose gradient direction is between 0° and 90° or 270° and 360°); on the contrary, South-facing stations showed positive residuals in all months, with values peaking in summer. So, facet effect was assumed to vary between π/2 and 3π/2, whereas for the other exposure angles the effect was assumed to be zero.

A more detailed analysis highlighted not only an obvious solar duration effect, but also an influence of the actual exposure, whose effects can be remarkably different when considering a purely Southward exposure rather than a South-West or a South-East exposure.

In order to capture the overall effect of facet exposure, the following model was created:

$$R_{facet} = -\alpha \sin(\frac{\pi}{2} - (facet))$$

where *facet* represents the direction of the gradient of *z (x,y)* and *α* is a monthly-dependent coefficient that represents the exposure effect concerning purely South-facing grid cells.

The monthly values of the *α* coefficient identified on the basis of a facet-based station residuals analysis and on knowledge-based considerations about the duration of the days in the different month are shown in fig. 16.

	Jan	Feb	Mar	Apr	May	Jun	Jul	Aug	Sep	Oct	Nov	Dec
α	0.4	0.5	0.6	0.7	0.8	0.9	0.8	0.7	0.6	0.5	0.4	0.3

Fig. 16 : Values of α coefficient for facet exposure effect

It is interesting to observe that the α values are approximately twice as big in summer than in winter: this result depends on the fact that in summer a South-facing station receives twice the solar radiation than a North-facing one.

Once the morphological (such as summit, valley and facet features) effects were defined, the approach adopted was similar to that described in chapter 3. Once more, it was

assumed to extend the station results to the grid cells; in particular, the procedure followed these steps:

a) for summit and valley grid cells, an effect equivalent to the average of the residuals of the corresponding cells with stations was assumed (obtained after the evaluation of the three leading geographical variables effects were removed);

b) for grid cells with facet between π/2 and 3π/2, an effect given by $R^{V}{}_{\mathrm{mod}\ el} = R_{facet} = -\alpha \sin(\frac{\pi}{2} - (facet))$ was assumed.

If the summit/valley and the facet effects are defined respectively by R^{IV} and R^{V}, it can be written:

$$T^{LM}{}_{\mathrm{mod}\ el} = T^{'''}{}_{\mathrm{mod}\ el} + R^{IV}{}_{\mathrm{mod}\ el} + R^{V}{}_{\mathrm{mod}\ el}$$

$$R^{LM}{}_{station} = R^{'''}{}_{station} - R^{IV}{}_{station\ \mathrm{mod}\ elled} - R^{V}{}_{station\ \mathrm{mod}\ elled}$$

where $T^{'''}{}_{\mathrm{mod}\ el}$ represents the estimation of the temperature by the geographical model including only the leading variables, $T^{LM}{}_{\mathrm{mod}\ el}$ represents the estimation of the temperature by the geographical model including the leading variables and the morphological effects (summit/valley and facet exposure effects) and $R^{LM}{}_{station}$ are the new residuals for every station after this step. A plot of this effect for January is shown in fig. 17.

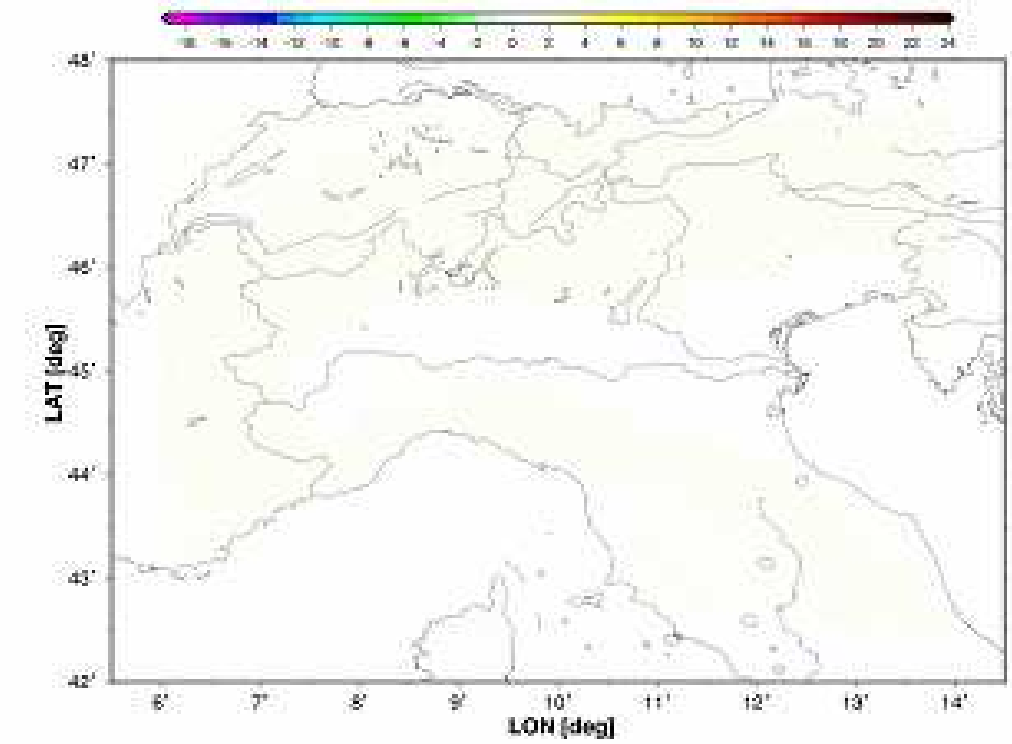

Fig. 17 : Map of facet exposure and summit/valley effects for January.

Even though the effects of the morphological variables were not as large as the leading effects and even though they only concerned a subset of the grid cells, a significant improvement in the model's skill resulted after the inclusion of these effects. The overall accuracy of the model, after this step, is shown in fig. 18.

	Jan	Feb	Mar	Apr	May	Jun	Jul	Aug	Sep	Oct	Nov	Dec	Average
ME	0.08	0.03	-0.07	-0.16	-0.19	-0.22	-0.26	-0.18	-0.06	0.05	0.06	0.08	*-0.07*
MAE	1.10	0.88	0.72	0.74	0.75	0.85	0.90	0.83	0.73	0.77	0.88	1.08	*0.85*
RMSE	1.40	1.12	0.92	0.94	0.96	1.08	1.15	1.05	0.93	0.99	1.12	1.38	*1.09*

Fig. 18 : Accuracy of the model including the dependence of temperature on the three leading geographical variables and on the morphological variables.

It is worth noticing that, at this point, the MAE is already below the threshold of 1 °C in every month, with the only exceptions of January and December; also the RMSE is below the threshold of 1 °C in five out of twelve months.

4.2 The sea effect (Part I: Ligurian, Tyrrhenian and North-Adriatic Seas)

The fifth step concerned the evaluation of the sea effect: a cooling sea effect in summer and a warming effect in winter were expected in the first kilometres inland from the coast. Moreover, a different behaviour of the different Italian coasts was expected according to knowledge of local climate patterns.

In order to evaluate the Sea effect in the area under examination, four separate zones were considered: Ligurian Sea (French Riviera, Liguria), Tyrrhenian Sea (Tuscany and northern Latium), North-Eastern Adriatic Sea (Friuli and Istria), South-Western Adriatic Sea (Veneto, Romagna and Marche). Such a separation is well justified by the geographical characteristics of the territory studied. Ligurian and Tyrrhenian Seas are both on the Western side of the Italian Peninsula, while the Adriatic Sea is on the Eastern side. Furthermore, the Adriatic Sea must be split into two sub-regions because the two areas

have a different coast exposure and the southern area is much more exposed to cold Eastward winds, especially in winter. Thus, in this step, Ligurian, Tyrrhenian and North-Eastearn Adriatic effects were studied, whereas South-Western Adriatic is discussed in chapter 4.5.

A sub-set of coast stations (only stations not farther than 60 kilometres from the coast) was selected in order to perform monthly linear regressions between the station residuals, obtained after taking into account the temperature dependence on the leading geographical variables and on the morphological variables, and the distance from the coast for every station of this sub-set. According to these definitions, 35 stations for Ligurian Sea area, 45 stations for Tyrrhenian Sea area and 30 stations for North-Eastern Adriatic Sea area were identified.

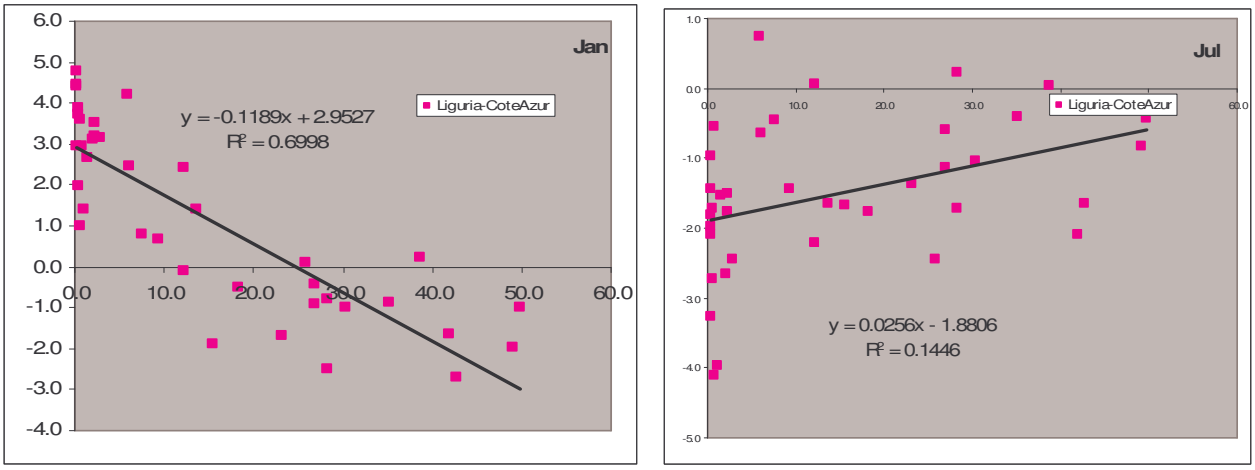

Fig. 19-20 : Temperature residuals (after taking into account the temperature dependence on leading geographical and on morphological variables) vs. distance from the Mediterranean coast for January and July.

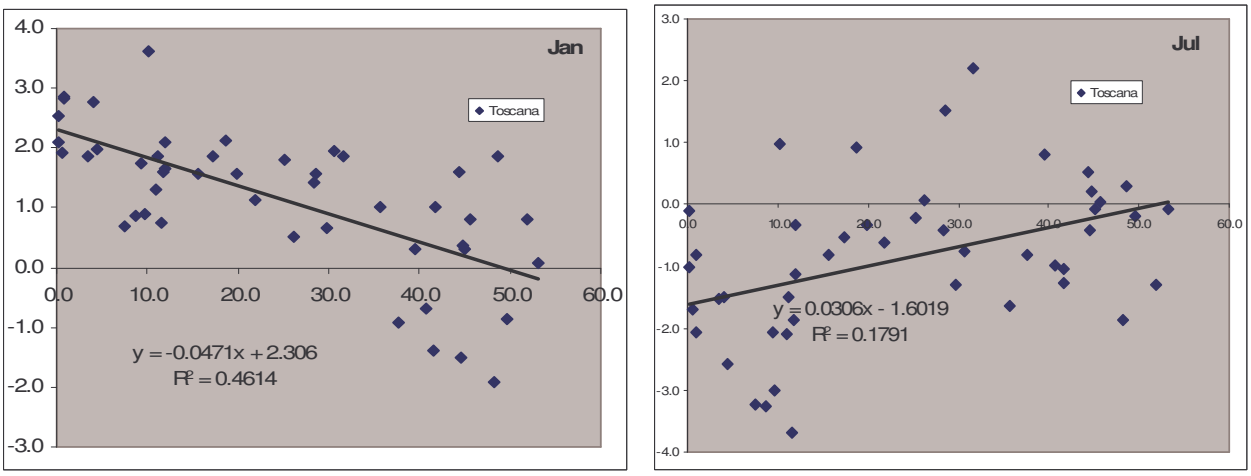

Fig. 21-22 : Temperature residuals (after taking into account the temperature dependence on leading geographical and on morphological variables) vs. distance from the Tyrrhenian coast for January and July.

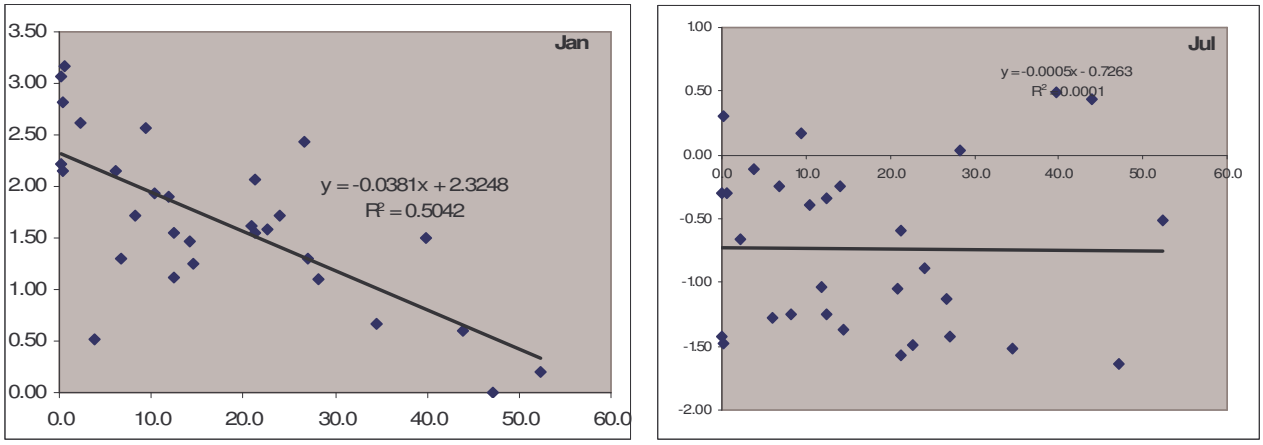

Fig. 23-24 Temperature residuals (after taking into account the temperature dependence on leading geographical and on morphological variables) vs. distance from the Adriatic coast for January and July.

Such a procedure can be summarized by the following two steps (it was used for each month, for each different Sea Area):

1.) From $R^{LM}{}_{stations}$ *at* 4^{th} *step* ⇨ *we found g, h from regression* $R^{LM}{}_{stations} = g(DistCoast)_{stations} + h$

2.) Using the same coefficients g, h ⇨ *we calculated* $R^{LMS}{}_{\mathrm{mod}\,el} = g(DistCoast)_{\mathrm{mod}\,el} + h$

where $R^{LM}{}_{stations}$ are the residuals after the evaluation of the leading geographical effects and of the morphological effects, $(DistCoast)_{stations}$ is the distance from the coast of the stations, $(DistCoast)_{\mathrm{mod}\,el}$ is the weighted distance from the coast of the grid cell. This weighted distance from the coast was based on a simple algorithm that sums up the linear distance from the nearest sea coast and the height differences (orographical obstacles) between the grid cell and the nearest sea coast (see fig. 25).

It was found a Sea effect for the Ligurian Sea of 3.1°C in January on the Ligurian coast (see fig. 19) and of -2.0°C for July (see fig. 20); it was found a Sea effect for the Thyrrenian Sea of 2.2°C in January on the Tuscan coast (see fig. 21) and of -1.6°C for July (see fig. 22); it was found a Sea effect for the North Adriatic Sea of 2.3°C in January on the Friulian Coast and Istria (see fig. 23) and of -0.7°C for July (see fig. 24).

Moreover, it was found that the Ligurian Sea and the Tyrrhenian Sea influence climate inland to 40 km from the coast, the North-Eastern Adriatic Sea to 60 km.

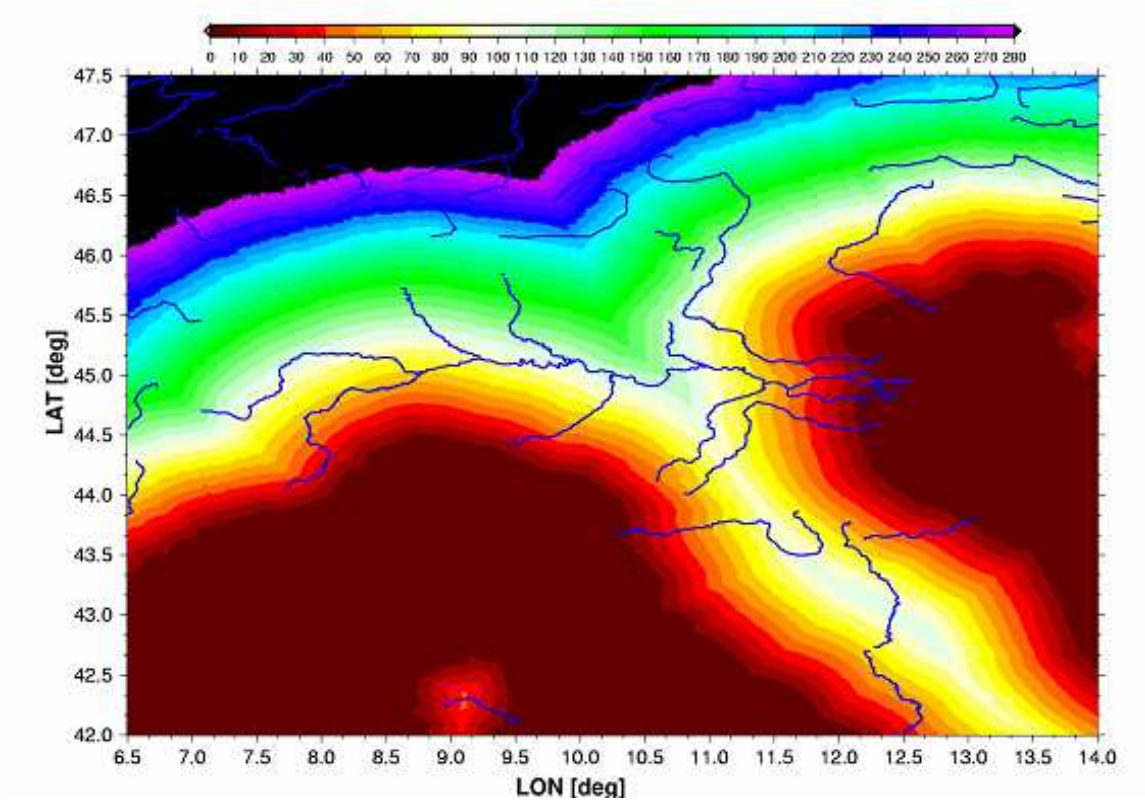

Fig. 25 : Weighted distance from the coast for the area under examination

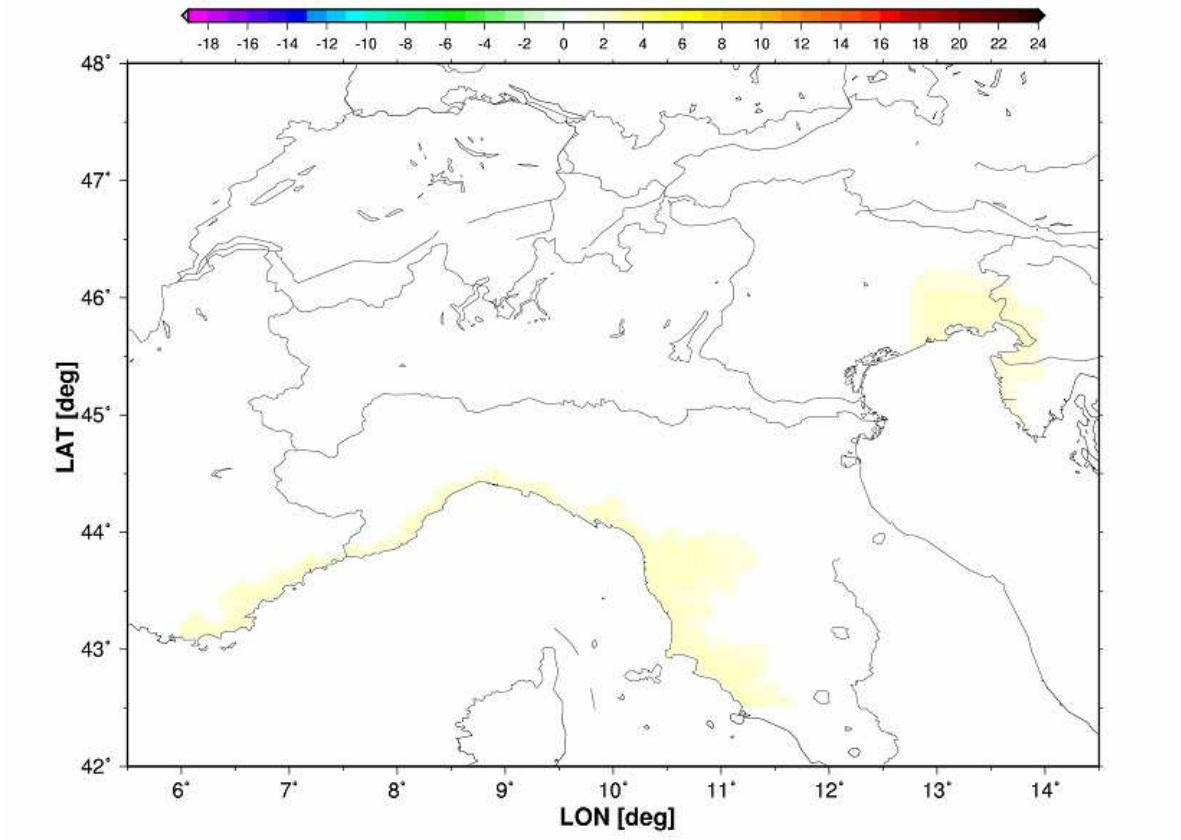

Fig. 26 : Warming sea effect (except South-Western Adriatic) for January.

The next step was the comparison between the modelled normal temperatures and the observed values. As in the previous steps, such a comparison was performed by studying the residuals.

In other words, the estimated temperature of each station according to the model including the elevation, the latitude, the longitude, the summit/valley, the facet exposure and the sea effects was calculated first and, secondly, the difference between the observed and modelled values for each station was calculated.

Such a procedure can be summarized by the following steps:

3.) Using g, h *,(DistCoast)station* ⇨ *we calculated back* $R^{LMS}{}_{station\,\mathrm{mod}elled} = g(DistCoast)_{station} + h$ *for each station*

4.)From $R^{LM}{}_{stations}$, $R^{LMS}{}_{station\ \mathrm{mod}\ elled}$ ⇨ *we calculated the new residual* $R^{LMS}{}_{station} = R^{LM}{}_{station} - R^{LMS}{}_{station\,\mathrm{mod}elled}$ *for each station*

5.) We used $T^{LMS}{}_{\mathrm{mod}\ el} = T^{LM}{}_{\mathrm{mod}\ el} + R^{LMS}{}_{\mathrm{mod}\ el}$ *for each grid cell of the considered area.*

The overall accuracy of the model shows a remarkable improvement in the statistical parameters (fig. 27).

	Jan	Feb	Mar	Apr	May	Jun	Jul	Aug	Sep	Oct	Nov	Dec	Average
ME	-0.16	-0.11	-0.09	-0.08	-0.07	-0.06	-0.10	-0.08	-0.05	-0.07	-0.13	-0.15	***-0.10***
MAE	0.93	0.80	0.72	0.73	0.72	0.78	0.82	0.81	0.73	0.71	0.77	0.93	***0.79***
RMSE	1.20	1.02	0.92	0.91	0.90	0.98	1.05	1.01	0.92	0.91	0.96	1.18	***1.00***

Fig. 27 : Accuracy of the model including the dependence of temperature on the three leading geographical variables, on the morphological variables and on the sea effect.

An intrinsic bias is still present, butbut e Sea effect. variables and

the MAE is now below the threshold of 1°C in every month, even in January and in December; the average RMSE is just equal to the threshold of 1°C and it is below the threshold in seven out of twelve months.

4.3 The Lake effect

The sixth step concerned the evaluation of the Lake effect: a slight cooling Lake effect in summer and a slight warming effect in winter were expected in the first kilometres inland from the lake coasts: the lake effect is very similar to the Sea effect, but it is a smaller effect and it decreases inland to a very small distance from the lake coast (not more than 5-10 km compared to 30-70 km for Sea effect).

In the geographical area under examination, 4 sub-Alpine (Maggiore, Lugano, Como, Garda) and 5 North-Alpine lakes (Zurich, Bodensee, Leman, Neuchatel, Vierwaldstattersee) were studied: each lake was studied separately.

As for the sea effect, a sub-set of "lake" stations (only stations not farther than 10 kilometres from the lake) was selected in order to perform monthly linear regressions between the station residuals, obtained after taking into account the temperature dependence on the leading geographical variables, on the morphological variables and on the sea effect, and the distance from the lake for every station of this sub-set. According to these definitions, only 25 lake stations were identified.

The same approach used for sea effect de-trending was adopted.

Such a procedure can be summarized by the following two steps (it was used for each month, for each lake):

1.) From $R^{LMS}{}_{stations}$ *at 5th step* ⇨ *we found i, j from regression* $R^{LMS}{}_{stations} = i(DistLake)_{stations} + j$

2.) Using the same coefficients i, j ⇨ *we calculated* $R^{LK}{}_{\mathrm{mod}\,el} = i(DistLake)_{\mathrm{mod}\,el} + j$

where $R^{LMS}{}_{stations}$ are the residuals after the evaluation of the leading geographical effects, of the morphological effects and of the Sea effect, $(DistLake)_{stations}$ is the distance from the lake of the stations, $(Distlake)_{\mathrm{mod}\,el}$ is the weighted distance from the lake of the grid cell calculated from the GTOPO30 (it takes into account the linear distance from the nearest lake, the elevation of the grid cell and the orographical obstacles between the grid cell and the nearest lake).

It was found that for Bodensee, Vierwaldstattersee and Neuchatel Lakes the lake effect is negligible and that the 4 lakes South of the Alpine ridge have very similar coefficients: so, the i, j coefficients were re-calculated and averaged for them.
For example, it was found on the Garda Lake coast, in January, a warming effect of approximately 1 °C , that is smaller than the Ligurian warming winter effect on French Riviera (approximately 2.6 °C / 3.2 °C) just on the coast.
The average residuals calculated for the lakes, related to the first kilometre from the lake coast, are shown in fig. 28.

	Jan	Feb	Mar	Apr	May	Jun	Jul	Aug	Sep	Oct	Nov	Dec	Average
Sub-Alpine Lakes	1.07	0.77	0.57	0.28	-0.13	0.07	0.18	0.31	0.46	0.69	0.72	1.11	**0.51**
Leman Lake	0.73	0.13	-0.59	-0.94	-1.02	-1.16	-1.12	-1.01	-0.75	-0.25	0.28	0.85	**-0.40**

Fig. 28 : Values of residuals at 1 km from the lake coasts.

The sub-Alpine Lakes (Maggiore, Como, Garda, Lugano), show a warming effect in winter that is stronger than the Leman Lake one, on the contrary the Leman Lake show a stronger cooling effect in summer; moreover the average yearly lake effect is a cooling effect for the Leman Lake and it is a warming effect for the 4 sub-Alpine lakes.

Once again, the next step was the comparison between the modelled normal temperatures and the observed values. As in the previous steps, such a comparison was performed by studying the residuals.

Such a procedure can be summarized by the following steps:

3.) Using i, j *,(DistLake)station* ⇨ *we calculated back* $R^{LK}{}_{station\,\mathrm{mod}elled} = i(DistCoast)_{station} + j$ *for each station*

4.)From $R^{LMS}{}_{stations}$, $R^{LK}{}_{station\ \mathrm{mod}\ elled}$ ⇨ *we calculated the new residual* $R^{LK}{}_{station} = R^{LMS}{}_{station} - R^{LK}{}_{station\,\mathrm{mod}elled}$ *for each station*

5.) We used $T^{LK}{}_{\mathrm{mod}\ el} = T^{LMS}{}_{\mathrm{mod}\ el} + R^{LK}{}_{\mathrm{mod}\ el}$ *for each grid cell of the considered area.*

The overall accuracy of the model shows a small improvement in the statistical parameters of the model (fig.29).

	Jan	Feb	Mar	Apr	May	Jun	Jul	Aug	Sep	Oct	Nov	Dec	Average
ME	-0.19	-0.12	-0.08	-0.07	-0.05	-0.04	-0.08	-0.07	-0.05	-0.07	-0.15	-0.18	*-0.10*
MAE	0.91	0.79	0.71	0.72	0.70	0.76	0.81	0.80	0.71	0.71	0.76	0.91	*0.78*
RMSE	1.18	1.02	0.91	0.90	0.89	0.97	1.04	1.00	0.91	0.90	0.95	1.17	*0.99*

Fig. 29 : Accuracy of the model including the dependence of temperature on the three leading geographical variables, on the morphological variables , on the Sea effect and on the lake effect.

4.4 The Po Plain cold air pool effect

By observing the winter residual distributions after the evaluation of the elevation, the latitude, the longitude, the Sea and the lake effects, it was noticed that in 5 months (from November to March) the stations located in the Po Plain have negative residuals, especially high from December to February. This is due to the inversion phenomena which frequently occur in the Po Plain lowlands and to the cold air masses stagnating in the Po Plain; furthermore, this effect is coupled with the longitude effect caused by continentality.
This phenomenon was not studied just considering the stations located in the Po Plain, but the area under this influence was enlarged towards South until Lat 42.5°E on the Eastern side of the Apennines, thus encompassing the area between the Adriatic coast and the Apennines beacuse the cold air masses effect is present not only in the Po Plain but even on the Adriatic coast in Romagna and Marche.
It was decided to model this effect considering also the elevation as a parameter, because, from the residuals obtained after the evaluation of the leading geographical variables, the morphological variables, the sea and the lake effects, a relation between such negative residuals and elevation was found: the residuals tended to decrease as the elevation increased.

From the analysis of the residuals, it was inferred that the inversion phenomena are not present in the Western part of Central Italy (that is the Tyrrhenian Sea coast, in fact Tuscany and Latium are generally warmer than Romagna and Marche in winter months).
In order to define the area influenced by the 'Po Plain' effect, only stations located at an elevation not higher than 600 m were considered: this threshold was chosen to include the hill area in the South-Western of Piedmont where the inversion phenomena are present. Another condition was added to model this effect: grid cells must have a slope value smaller than 0.15: thus hill sides and Pre-Alps were excluded because air masses can only station on locally flat areas.
According to these conditions 105 stations were selected for the analysis.

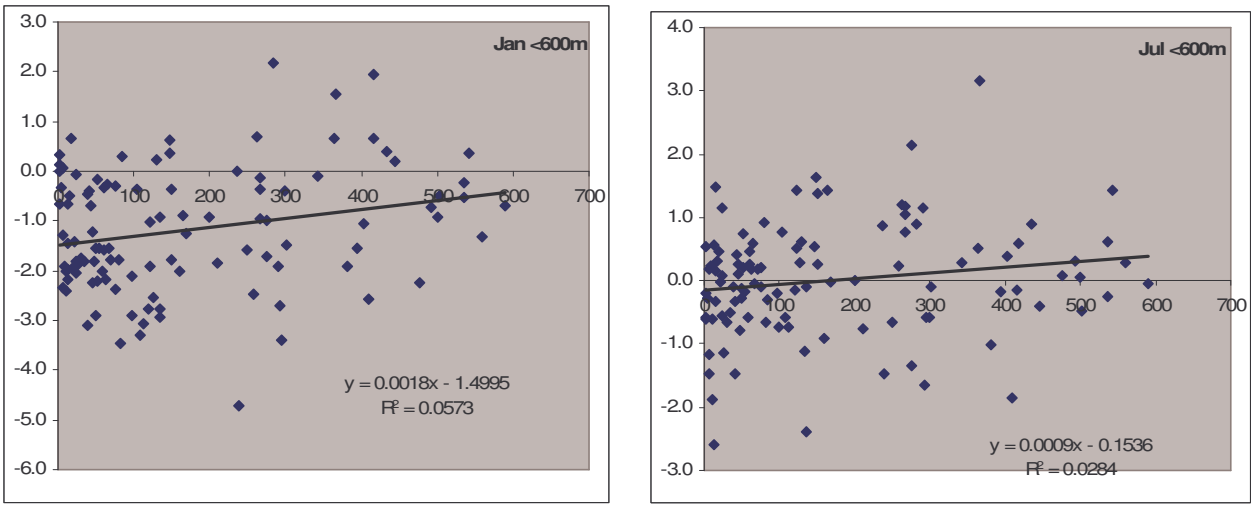

Fig. 30-31 : Temperature residuals (after taking into account the temperature dependence on leading geographical on morphological variables, on Sea and lake effects) vs. elevation in the Po Plain area for January and July.

Such a procedure can be summarized by the following two steps (it was used for every month):

1.) From $R^{LK}{}_{stations}$ *at 6th step* ⇨ *we found l, m from regression* $R^{PP}{}_{stations} = l(elev)_{stations} + m$

2.) Using the same coefficients l, m ⇨ *we calculated* $R^{PP}{}_{\mathrm{mod}\ el} = l(elev)_{\mathrm{mod}\ el} + m$

where $R^{PP}{}_{stations}$ are the residuals after the evaluation of the leading geographical effects, of the morphological effects and of the Sea end the lake effects, $(elev)_{stations}$ is the elevation

of the stations, $(elev)_{\mathrm{mod}\,el}$ is elevation the of the grid cell from GTOPO30 digital elevation model (it is the average elevation of the cell, not the elevation of the grid cell's centre).
It was found that this effect is noteworthy in five months: from November to March (e.g. -1.4 °C at 5 m in January), whereas in late spring, in summer and in early autumn months this effect is negligible (see fig. 30-31).
Another interesting result is that in the proximity of the coast, in winter, the warming sea effect prevails against the cold air masses effect up to 5 kilometres from the coast in Veneto and in Romagna.

As the same, it was evaluated the comparison between the modelled normal temperatures and the observed values by studying the residuals.

Such a procedure can be summarized by the following steps:

3.) Using l, m, (elev)station ⇨ we calculated back $R^{PP}{}_{station\,\mathrm{mod}\,elled} = l(elev)_{station} + m$ *for each station*

4.)From $R^{LK}{}_{stations}$, $R^{PP}{}_{station\ \mathrm{mod}\ elled}$ ⇨ *we calculated the new residual* $R^{PP}{}_{station} = R^{LK}{}_{station} - R^{PP}{}_{station\,\mathrm{mod}elled}$ *for each station*

5.) We used $T^{PP}{}_{\mathrm{mod}\ el} = T^{LK}{}_{\mathrm{mod}\ el} + R^{PP}{}_{\mathrm{mod}\ el}$ *for each grid cell of the area under examination.*

After the evaluation of the so-called Po Plain effect, statistical parameters of the model show an improvement (see fig. 32).

	Jan	Feb	Mar	Apr	May	Jun	Jul	Aug	Sep	Oct	Nov	Dec	Average
ME	0.00	0.01	-0.02	-0.07	-0.05	-0.04	-0.08	-0.07	-0.05	-0.07	-0.03	-0.01	***-0.04***
MAE	0.84	0.75	0.69	0.72	0.70	0.76	0.81	0.80	0.71	0.71	0.72	0.85	***0.76***
RMSE	1.08	0.96	0.89	0.90	0.89	0.97	1.04	1.00	0.91	0.90	0.91	1.08	***0.96***

Fig. 32 : Accuracy of the model including the dependence of temperature on the three leading geographical variables, on the morphological variables , on the Sea effect, on the lake effect and on the Po Plain effect.

The most important refinement is the removal of the intrinsic bias for winter months, in fact ME is null, e.g., for January. The average MAE and RMSE are both below the 1 °C threshold.

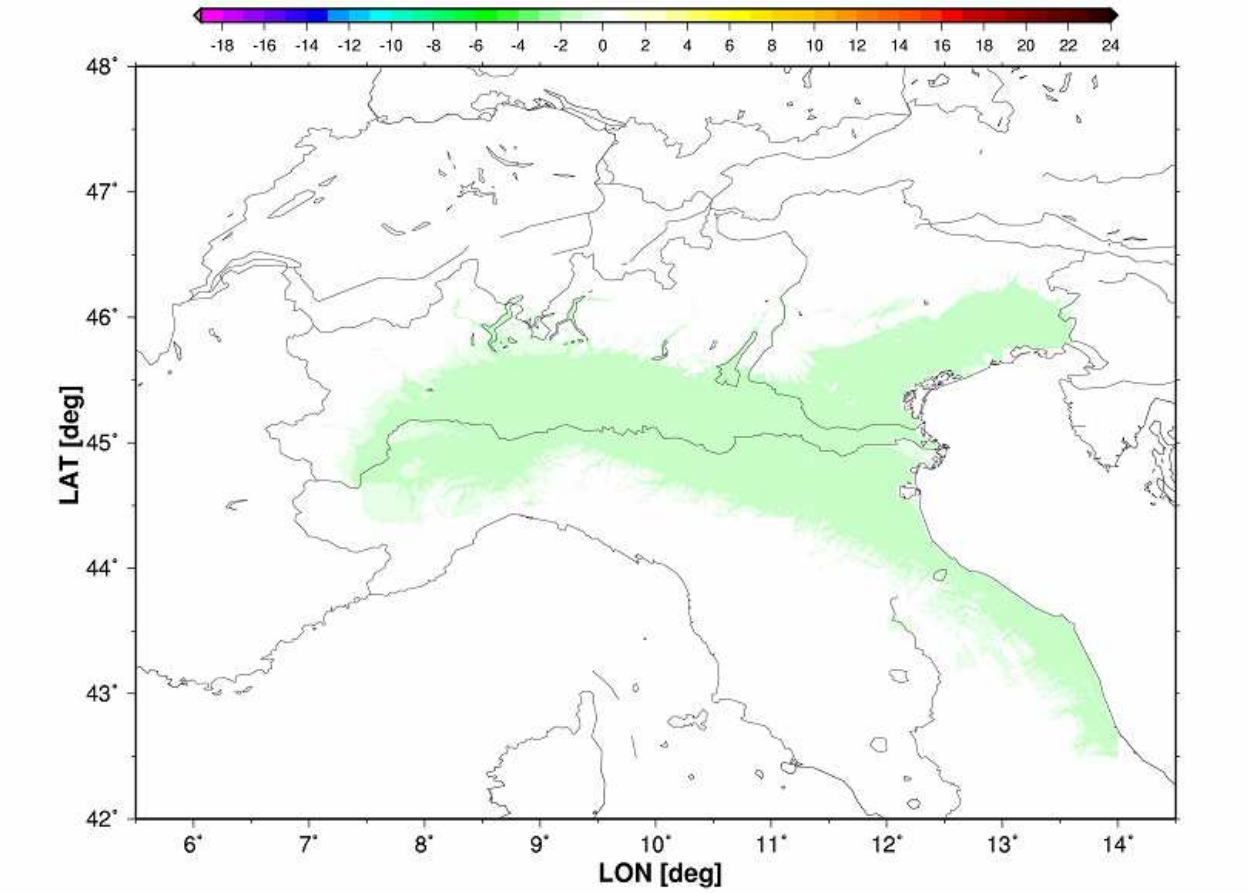

Fig.33 Po Plain cold air masses effect for January

Some further considerations: small geographical corrections (the effect was dampened as Latitude decreases, below 44°N) were introduced to create a model that reproduce in the most accurate way the station data (see fig. 33).

The model was created considering a one-layer atmosphere: in general, this could lead to a wrong evaluation of temperatures in the first 500 meters. In this case, the Po Plain inversion effect corrects this intrinsic problem.

In order to compare the results obtained after the inclusion of the Po Plain effect in the one-layer model with the results that it would be obtained if it had been used a two-layer atmosphere (elevation split threshold at 1500 m), such a two-layer model was applied.

It was found that the model described in this report (i.e. the one-layer atmosphere model plus the Po Plain effect in five months) is more similar to station data than the two-layer model: in fact, the overall accuracy of the statistical parameters show is better for the one-layer atmosphere model, the average MAE is lower (0.75 versus 0.9), and also the RMSE is lower (0.95 versus 1.15).

4.5 The Sea Effect (Part II: South-Western Adriatic Sea)

The seventh and last step concerned the evaluation of the South-Western Adriatic Sea effect: as for the other seas in the area studied, a cooling Sea effect in summer and a warming effect in winter are expected in the first kilometres inland from the coast.
The conditions for the station selection were the same adopted in chapter 4.2, thus we selected 20 stations for this analyses.
The residuals (for the selected stations) obtained after the evaluation of the temperature dependence on the three geographical and the morphological variables, of the Sea, the lake and the so-called Po Plain effect were studied in order to analyze their dependence on the distance from the South-Western Adriatic Coast with a linear regression performed for every month (see fig. 34 for January and fig. 35 for July).

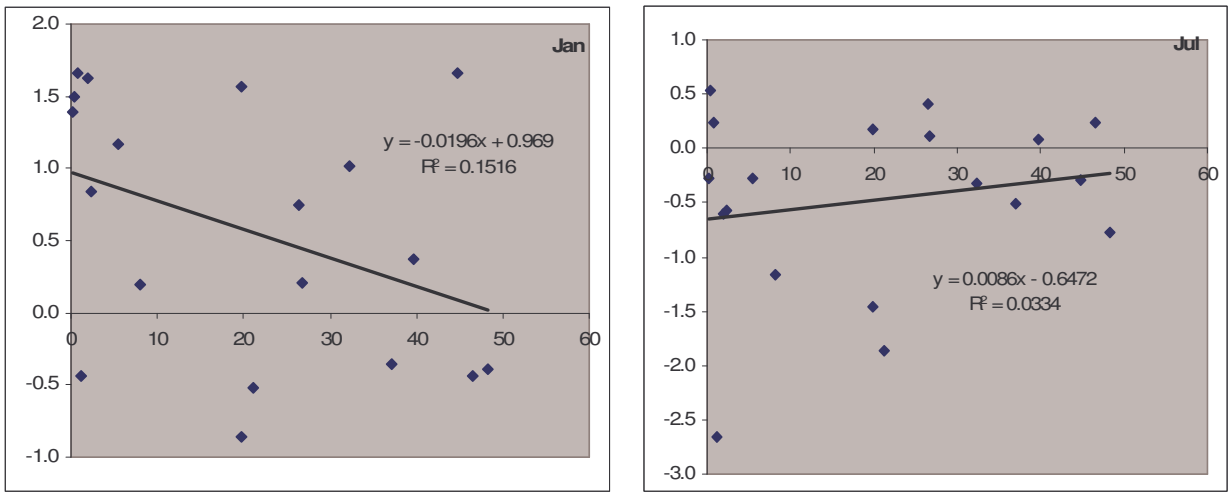

Fig. 34-35 : Temperature residuals (after taking into account the temperature dependence on leading geographical on morphological variables, on Sea, on lake and on the Po Plain effects) vs. distance from the South-Western for January and July

The procedure is formally the same explained in chapter 4.2, and it can be summarized by the following two steps (it was used for every month):

1.) From $R^{PP}{}_{stations}$ *at 7th step* ⇨ *we found o, p from regression* $R^{AS}{}_{stations} = o(DistCoast)_{stations} + p$

2.) Using the same coefficients o, p ⇨ *we calculated* $R^{AS}{}_{\mathrm{mod}\,el} = o(DistCoast\ )_{\mathrm{mod}\,el} + p$

where $R^{PP}{}_{stations}$ are the residuals after the evaluation of the leading geographical effects, of the morphological effects and of the other effects already evaluated, $(DistCoast)_{stations}$ is the distance from the coast of the stations, $(DistCoast)_{\mathrm{mod}\,el}$ is the weighted distance from the coast of the grid cell. This weighted distance is the one used in chapter 4.2 (see fig. 25).

It was found a Sea effect for the South-Western Adriatic Sea of 1.0 °C in January on the Marche coast (see fig. 34) and of -0.6 °C for July (see fig. 35), moreover the South-Western Adriatic Sea influences climate inland up to 40 kilometres (see fig. 36)

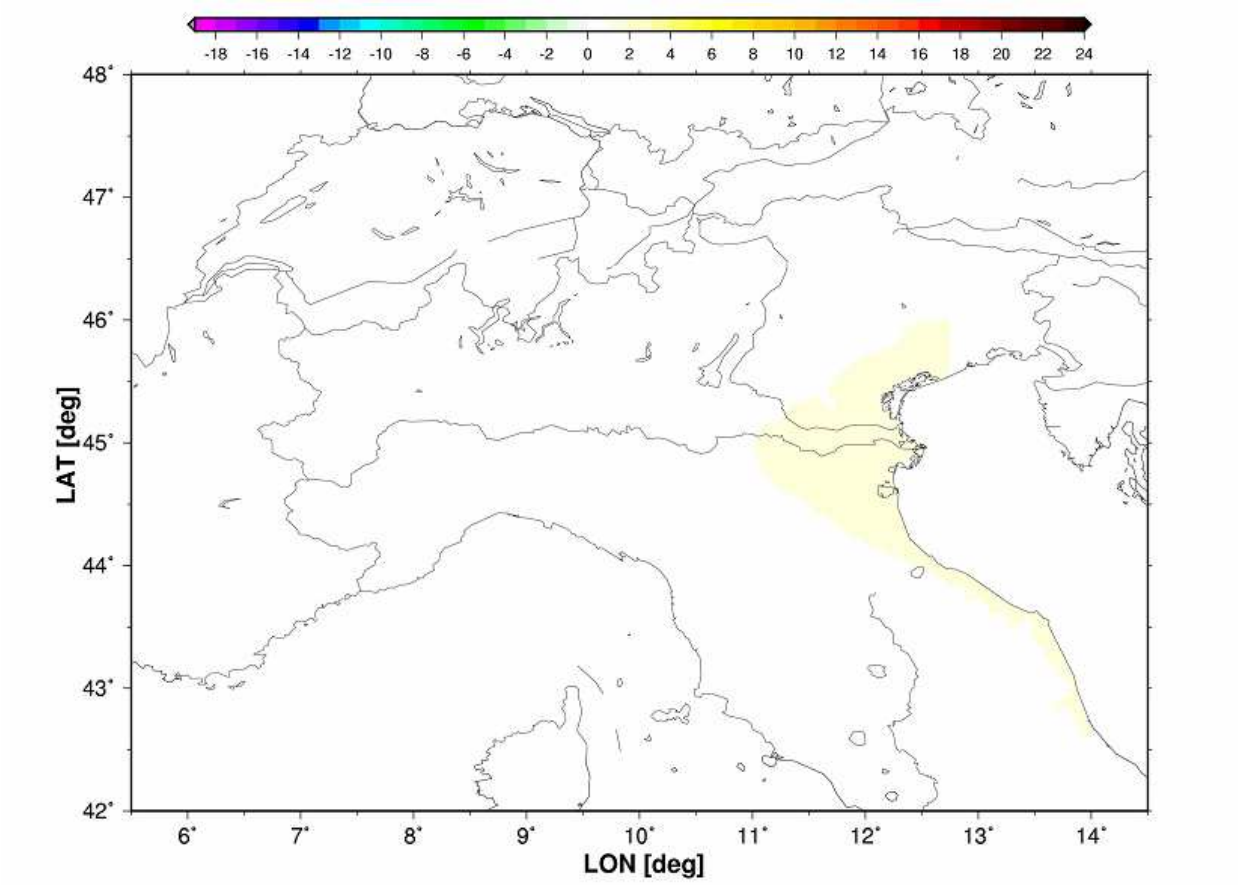

Fig.36 South-Western Adriatic Sea warming winter effect for January

Temperatures measured in Marche are hotter than in Veneto, because of a less intense Po Plain cooling effect in winter and because of the Latitude effect. The main difference between North-East Adriatic influence and the South-West one is the smaller cooling

summer effect: this probably depends on the Alps that are an orographical barrier against cold weather fronts for the Northern part of the Adriatic Sea.

Once again, the next step was the comparison between the modelled normal temperatures and the observed values. As in the previous steps, such a comparison was performed by studying the residuals.
Such a procedure can be summarized by the following steps:

3.) Using o, p, (DistCoast)station ⇨ we calculated back $R^{AS}{}_{station\,\mathrm{mod}elled} = o(DistCoast)_{station} + p$ *for each station*

4.)From $R^{PP}{}_{stations}$, $R^{AS}{}_{station\ \mathrm{mod}\ elled}$ ⇨ *we calculated the new residual* $R^{SS}{}_{station} = R^{PP}{}_{station} - R^{AS}{}_{station\,\mathrm{mod}elled}$ *for each station*

5.) We used $T^{SS}{}_{\mathrm{mod}\ el} = T^{PP}{}_{\mathrm{mod}\ el} + R^{AS}{}_{\mathrm{mod}\ el}$ *for each grid cell of the considered area.*

$R^{SS}{}_{station}$ and $T^{SS}{}_{model}$ are, respectively, the final residuals for every station and the final temperature values for every grid cell.
Such quantities were used to calculate the final statistical parameters of the climatological model, thus the overall final accuracy of the model is shown in (fig. 37).

	Jan	Feb	Mar	Apr	May	Jun	Jul	Aug	Sep	Oct	Nov	Dec	Average
ME	-0.04	-0.02	-0.03	-0.06	-0.05	-0.04	-0.08	-0.07	-0.06	-0.09	-0.05	-0.04	***-0.05***
MAE	0.83	0.74	0.69	0.71	0.70	0.76	0.81	0.79	0.71	0.70	0.71	0.83	***0.75***
RMSE	1.06	0.96	0.89	0.90	0.89	0.96	1.03	1.00	0.91	0.90	0.90	1.07	***0.95***

Fig. 37 : Final accuracy of the model including the dependence of temperature on every geographical, morphological and physical effect considered.

A small negative bias in winter months is present, but the geographical MLR model satisfies the error thresholds (MAE and RMSE are smaller than 1 °C); these parameters evaluation substitutes a jack-knife cross validation.

5. Future improvements

5.1 The Urban Heat Island Effect

It is well known that big cities (more than 50,000 inhabitants and population density at least 300 inhab/km^2) can cause an urban heat island especially in winter, during calm nights with clear sky (Oke, 1973; Oke, 1982).

In this study 25 urban stations in the Italian area were considered and linear regressions between temperature residuals versus population (number of inhabitants), versus the logarithm of population (as some papers suggest), versus density of population, versus the logarithm of density were performed. The results did not show a clear urban heat island (UHI) effect.

Maybe this is due to an incorrect classification of the stations: in the HISTALP database there are stations labelled as “urban” that are located a few kilometres away from the cities or, in some cases, the stations are located in airports which are not in the urban area (Milan Malpensa station is an example of that misleading label).

Another reason that may cause this difficulty in clearly detecting the UHI effect may be due to the fact that this phenomenon has a very local scale which is linked to features like the materials used for buildings, the canyon-free factor, the sky-view factor and so on.

Therefore, the characteristic spatial scale of the UHI is the micro-scale. Such a scale is unfortunately very hard to be captured with the HRT HISTALP database which has, on one hand, a low spatial density of stations and, on the other hand, a not sufficiently precision (less than 50 m) in the latitude and longitude geographical coordinates of the stations, thus causing problems to determine the right position of all stations.

Anyway, in spite of all these problems, it was decided to include in the HRT climatologies a first and very preliminary evaluation of the UHI effect. Such an estimate was based on regressions of the temperature residuals obtained after considering all the effects already described in this report, versus population. The regressions were not only performed for

the Italian area, but for the entire GAR, selecting three groups of stations (stations with a population between 50,000 and 500,000 inhabitants, between 500,000 and 1,000,000, more than 1,000,000). The preliminary results show that the UHI effect varies with density of population: it ranges, for towns between 500,000 and 1,000,000 inhabitants, from 0.4 °C to 0.9 °C in winter and from 1.3 °C to 2.2 °C in summer.

The inclusion of the UHI effect does not the improve statistical parameters of the model described in this report. The ME and the RMSE does not change, and the MAE improves only 0.01 °C.

In order to better consider the urban heat island effect in an oncoming future, it would be helpful a better localization and choice of “urban” station will be necessary and it will probably be useful taking into account not only the land cover value associated to the grid cell where a temperature station is located, but also the land cover values of the surroundings grid cells (8 cells at least) and, in the end, analyses based on couples of urban versus rural stations located no more than 25 km from one another can probably give a more detailed study of the UHI effect.

5.2 The Land Cover / Land Use Characterization

In recent literature no papers trying to include land cover in construction of hig resolution temperature climatologies were found. In order to evaluate a land cover effect, a high resolution and updated land cover data set, a great number of stations and a very efficient code to perform the analyses are requested. There are two different land cover grids useful for the GAR area.

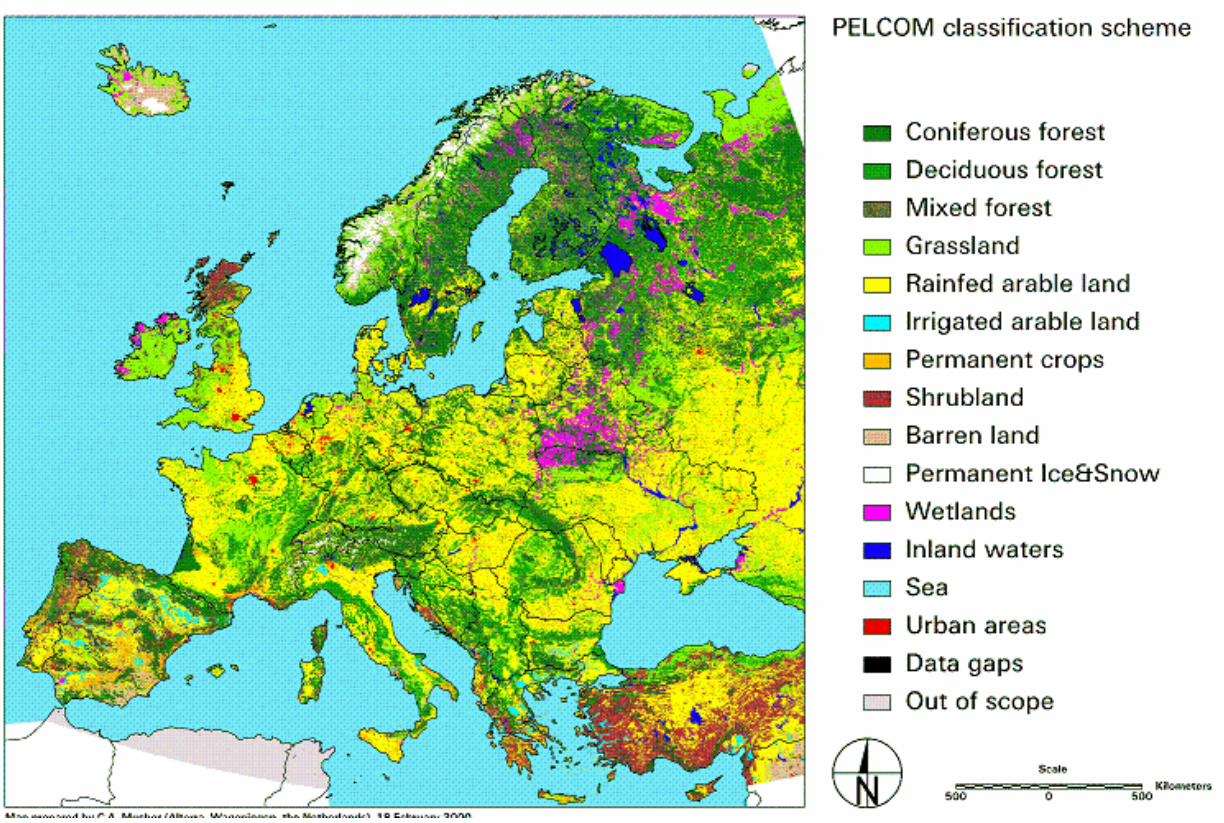

Fig. 38 : PELCOM Land Cover Data for Europe (1 km^2 resolution) and classification scheme.

This first one is PELCOM Land Cover pan-European database (fig. 38), it is data updated to 2001 and this is not the best solution for 1961-90 climatologies. The data are projected using Albers Conical Equal Area projections, the resolution is 1 km^2 for each grid cell.

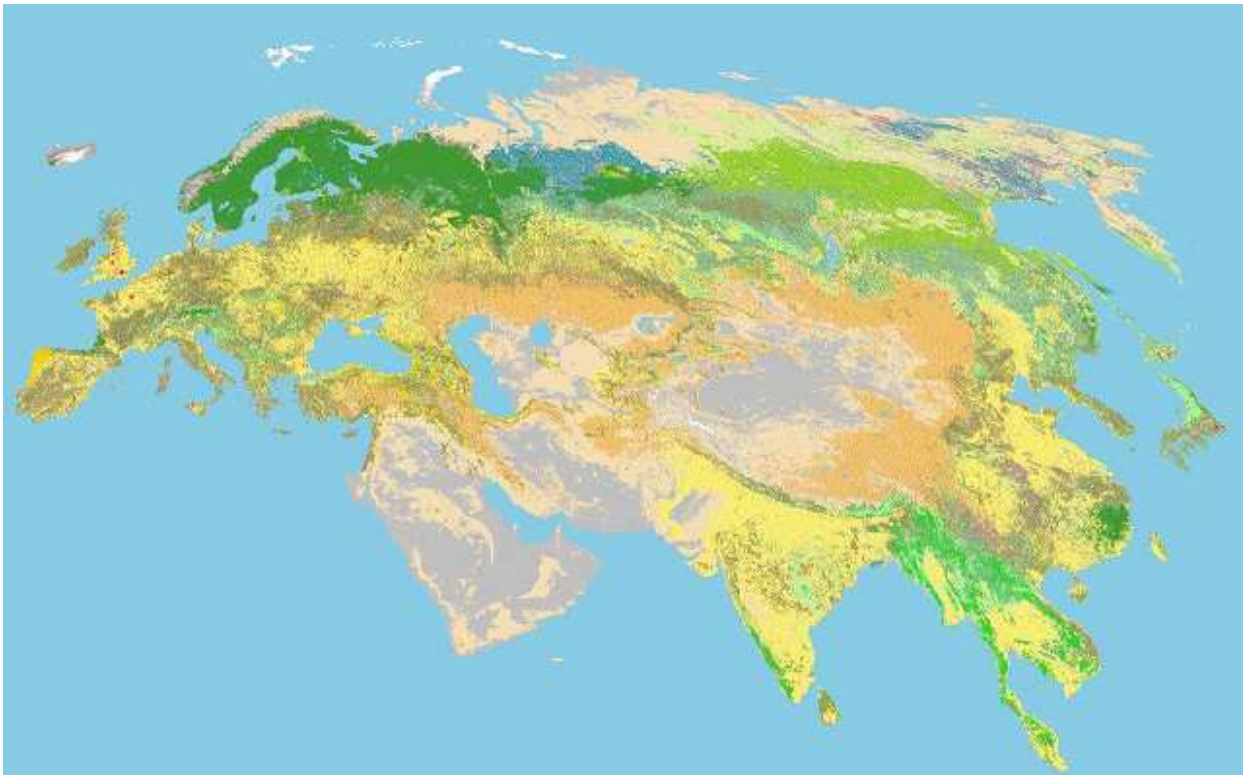

Fig. 39 : USGS Land Cover Data for Europe and Asia (1km resolution)

The second one is USGS Land Cover Eurasia database (fig. 39), it is updated to 1993. The data are projected using Interrupted Goode Homolosine projections or Lambert Azimuthal Equal Area projections, and its spatial resolution is 1 km^2 for each grid cell.

A great number of stations is needed to evaluate the land cover effect, because a significant number of station data should be associated to each kind of land cover. Each station is located in a grid cell with its land cover value (which corresponds to a different land type, for example deciduous forest, grassland, shrub land and so on), then data stations will be joined into small groups (one group for every land cover type).

The classification scheme of PELCOM land cover database has 14 land cover categories: at least, for each category, 20 stations are needed (but 50 would be preferable). The model described in this report is based on 664 stations, thus the HISTALP database has enough stations to perform a land cover study for the Northern part of Italy. On the other side, the USGS land cover scheme has more than 20 land cover different categories: in this case it will be necessary to perform the data analysis using a greater area (the whole GAR with their 1750 stations) because a greater number of temperature stations is needed.

It can be supposed that a land cover effect evaluation will significantly improve the model, even though the benefits of the use of land cover data can be estimated only in future works.

6. Results: HRT monthly maps for 1961-90

6.1 The Fortran code

A Fortran program with a simple structure was encoded (with a subroutine for each effect) and it was used to pass from residual data and temperature modelled values for each station to gridded temperature climatologies. Twelve short (from 450 to 650 code lines, it depends on the number of effects considered, for example in winter months there is no Po Plain effect) programs were written (one for each month) and one for the average temperature climatology. The thirteen programs final run did not take more than 30 minutes: fast Fortran codes were created to produce our final model with gridded data (the so called climatologies). Thus station data were converted into continuous gridded data.
Then it was used GMT (Generic Mapping Tools, a free software available online thanks to Honolulu University, department of Geophysics) to create the temperature maps.

6.2 Final statistical parameters and discussion

The final ME is -0.05 °C, an intrinsic negligible negative bias; the final MAE is 0.75 °C; the final RMSE is 0.95 °C. Such values were found just evaluating the final temperature residuals (measured values minus final modelled values), whereas a jack-knife cross validation was not performed.
No station was rejected, if only 5% of the data (the stations with the highest, negative or positive final residuals), had been rejected, the model would have had better statistical parameters (ME -0.03 °C, MAE 0.67 °C, RMSE 0.77 °C) but it would have been less realistic.

If the final averaged residuals of our model are plotted in monthly maps, there are only two areas where the average station residuals are larger than 1.0 °C: the South West of Piedmont (Langhe and Monferrato) in winter and the Adige (Etsch) Valley in winter and summer. The South-Western Piedmont is hotter than reality, because the Po Plain effect was modelled with a linear regression between temperature and elevation: this area is located at approximately 500 m, thus the effect in the model is not well captured even though that area has a rather continentality. In the Adige Valley there are 5-7 stations with very highly negative residuals (about -2.5 °C) in winter and very highly positive ones (more than 2.0°C) in summer: this is probably due to the remarkable inversion effects in Adige Valley and in secondary valleys in that area. Also this effect is probably caused by the high continentality effect that is not properly captured by the model. A third area with significantly negative residuals was found, the Bernese Oberland: this are is all the year round hotter in the model than in reality: this is a very cold area (approximately 0.8°C every month), probably because this is an area particularly exposed to the Atlantic cold weather fronts.

Finally, the statistical parameters only for the Italian stations were evaluated: the result is a little bit worse because the model was planned for a bigger area: ME is 0.11°C and it means that the intrinsic negative bias for our model is caused by some cold areas over the Alps, MAE is 0.79°C and RMSE is 1.01°C.

6.3 HRT monthly 1961-60 maps

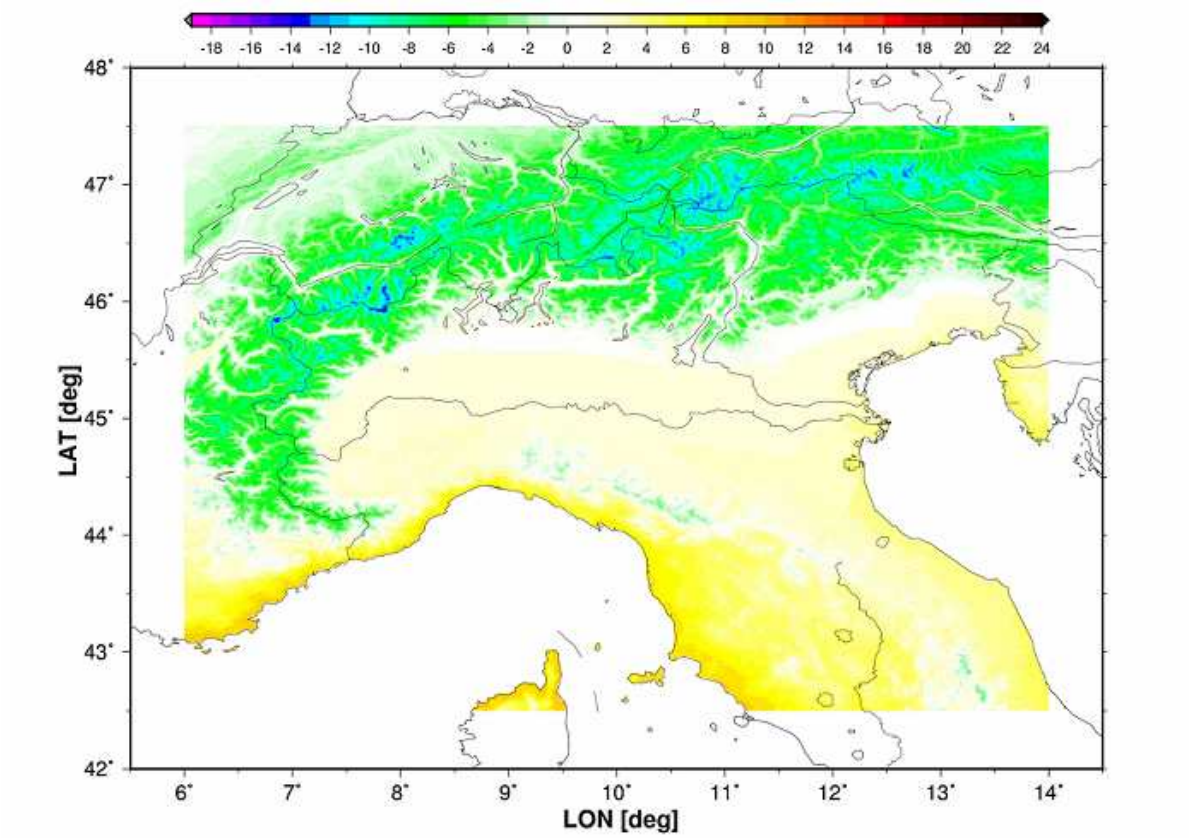

Fig. 40 : January temperature map.

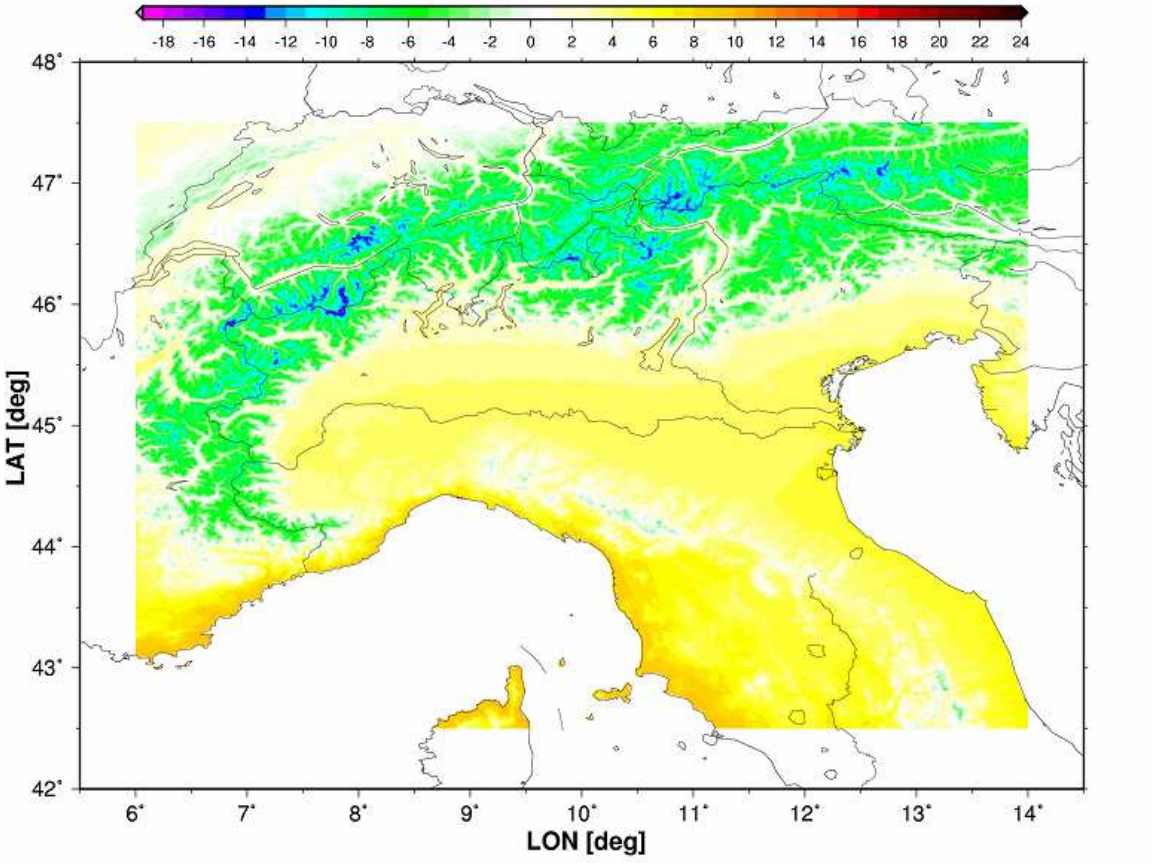

Fig. 41 : February temperature map.

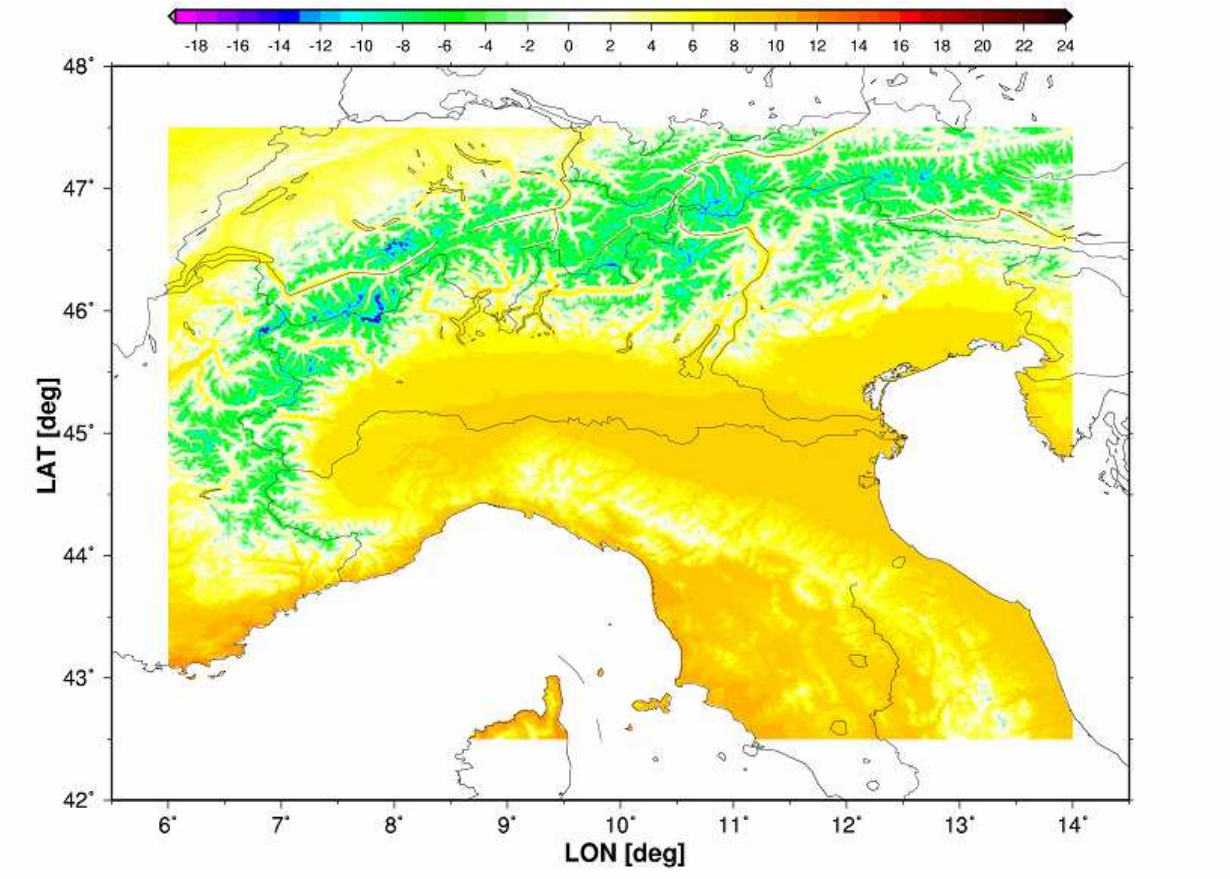

Fig. 42 : March temperature map.

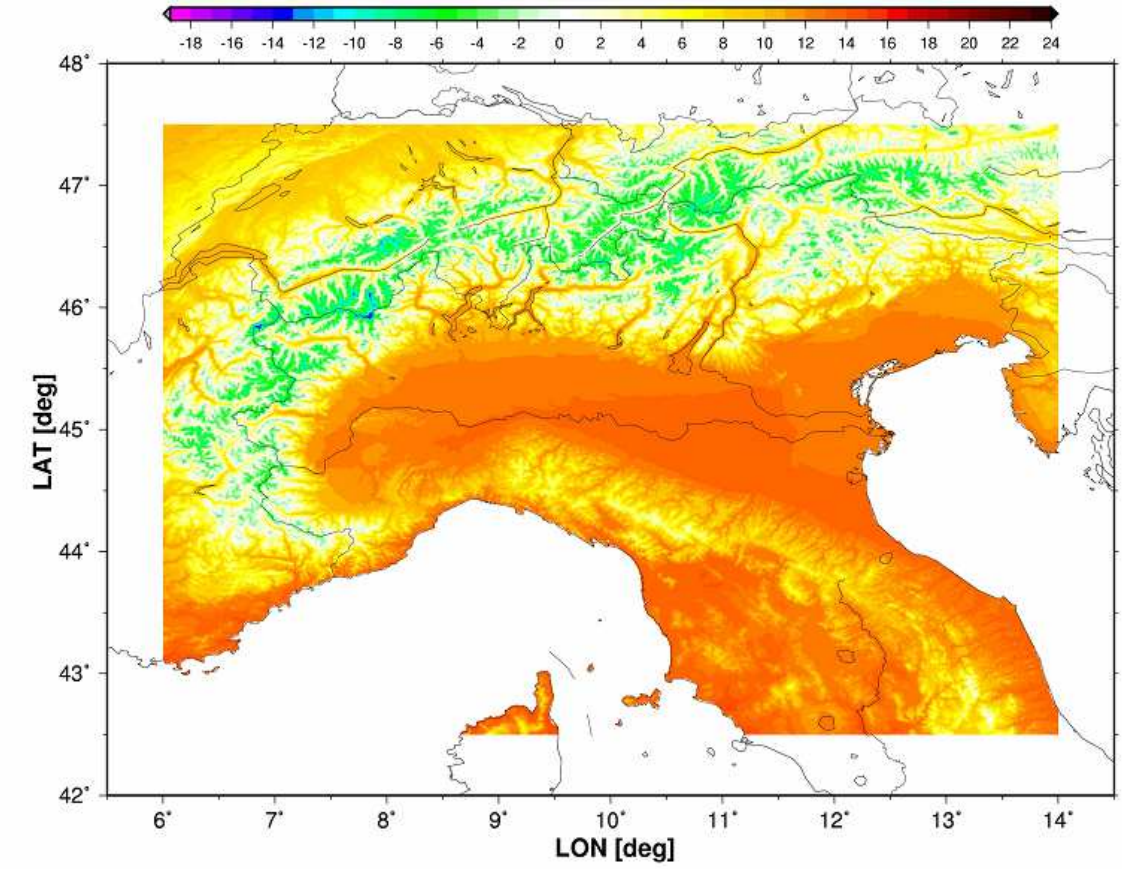

Fig. 43 : April temperature map.

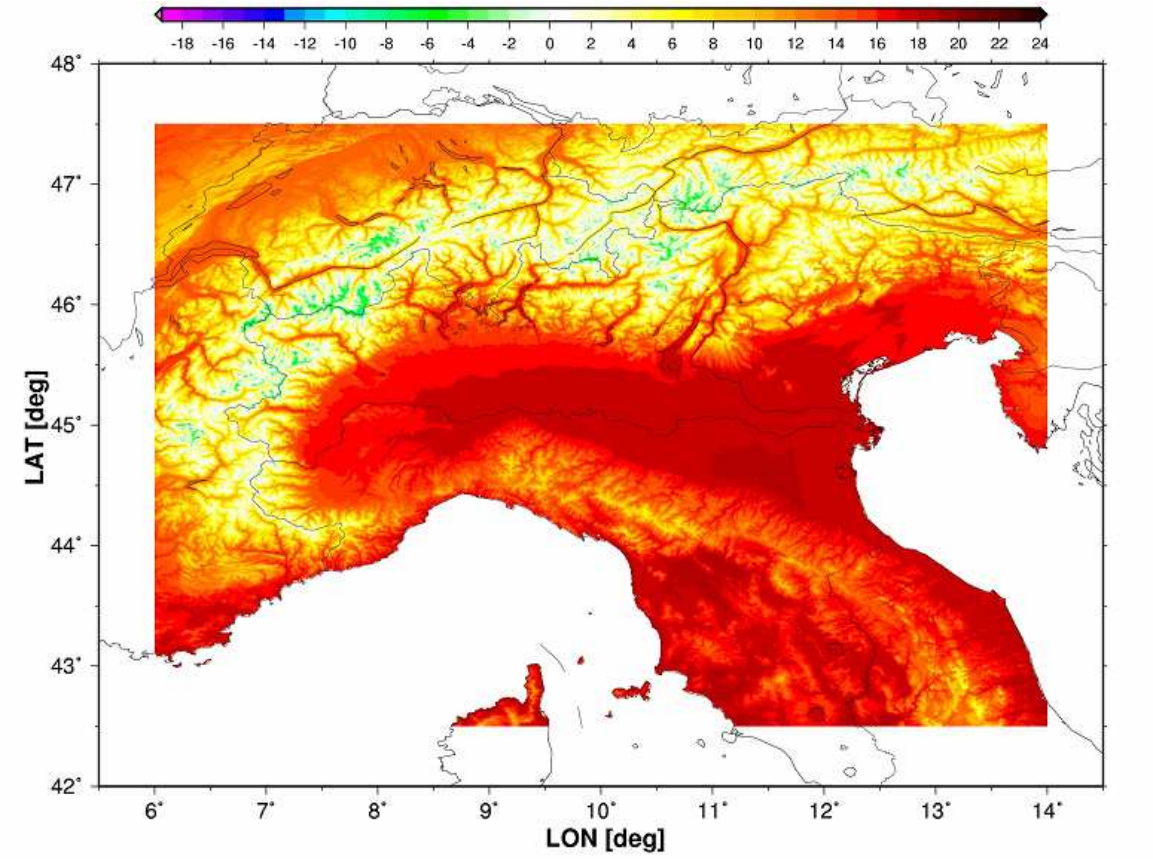

Fig. 44 : May temperature map.

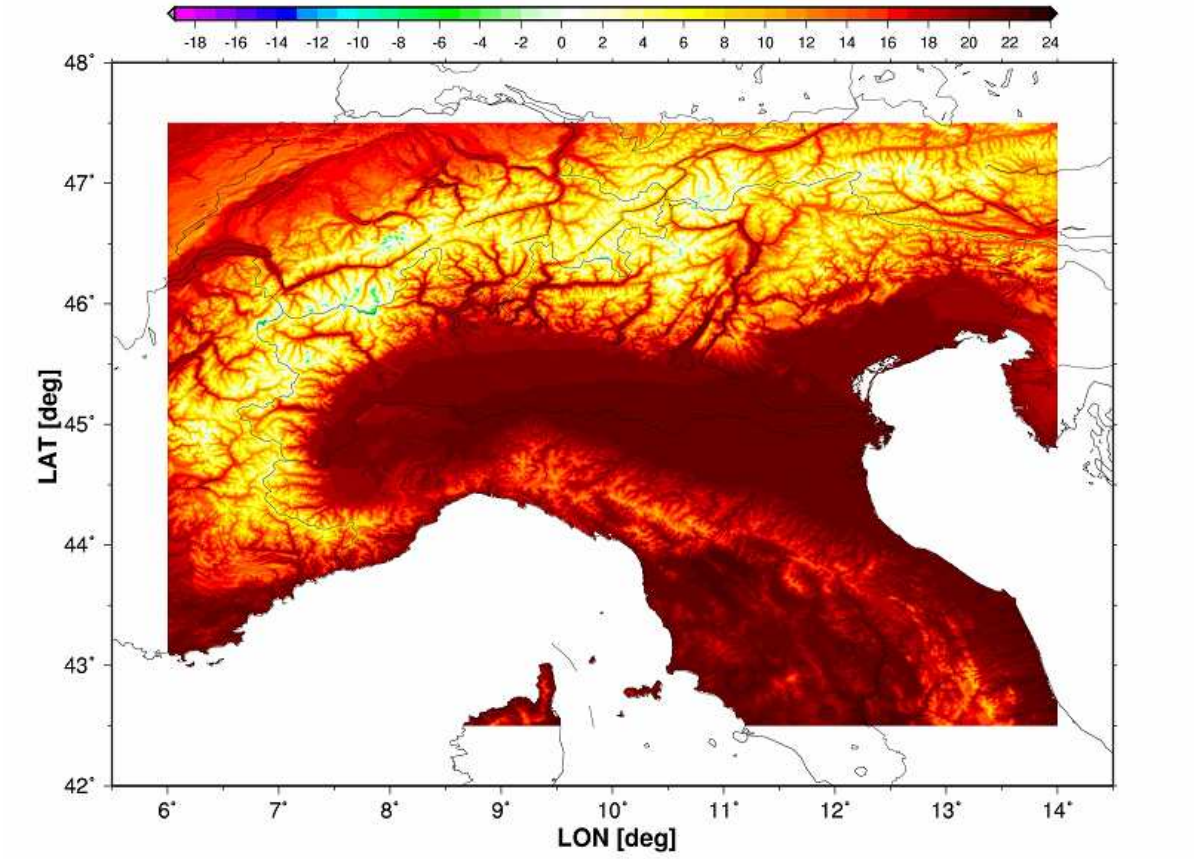

Fig. 45 : June temperature map.

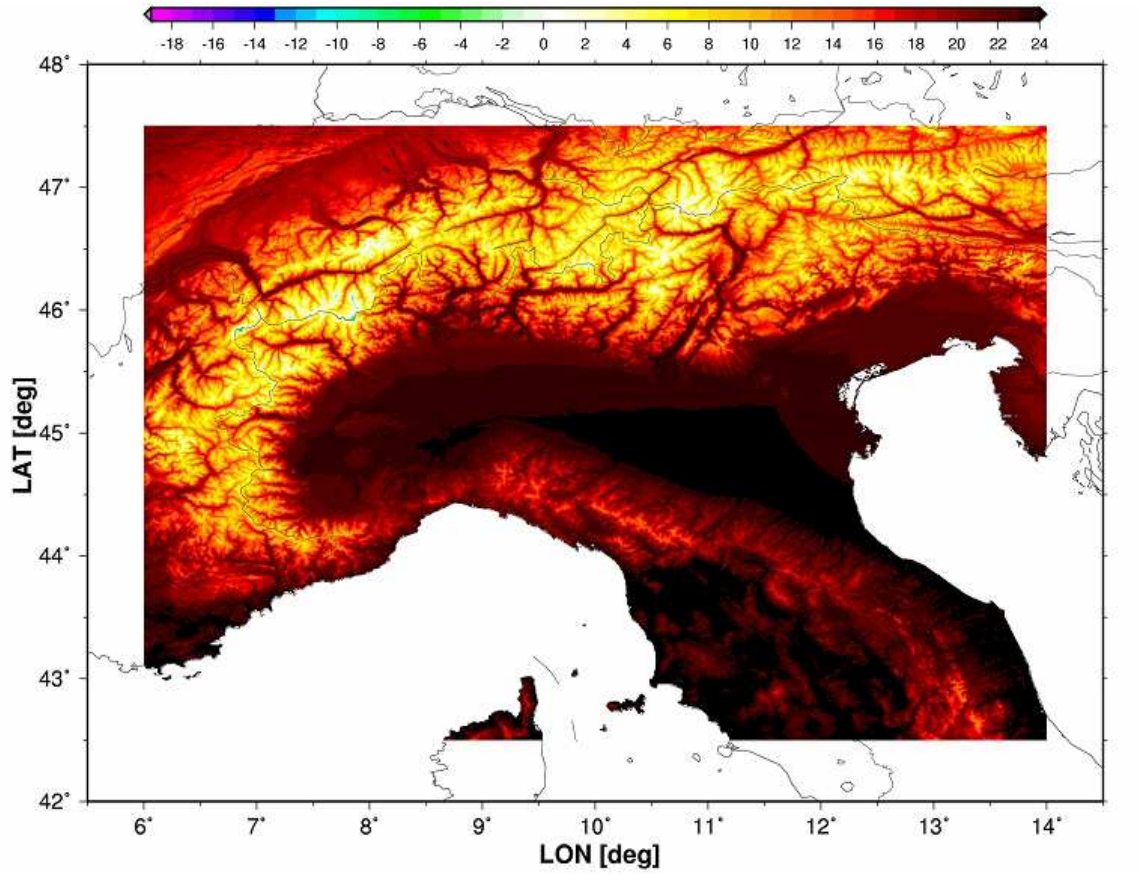

Fig. 46 : July temperature map.

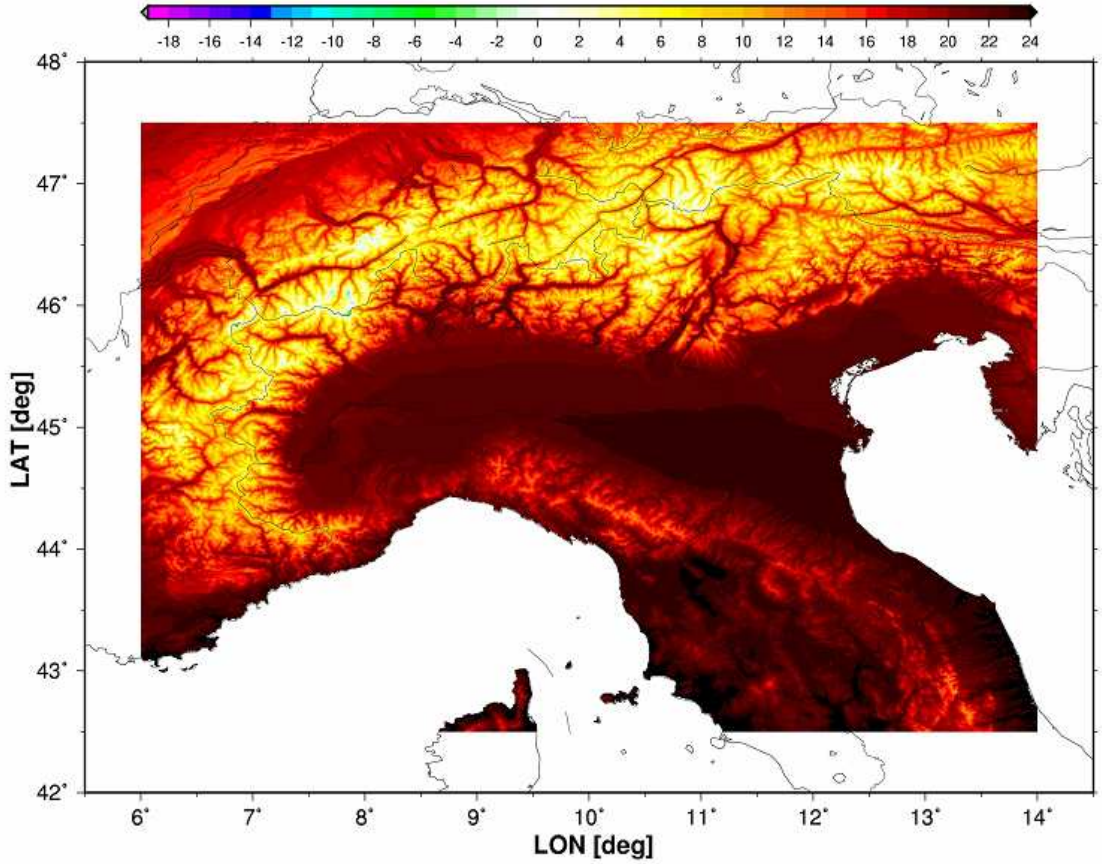

Fig. 47 : August temperature map.

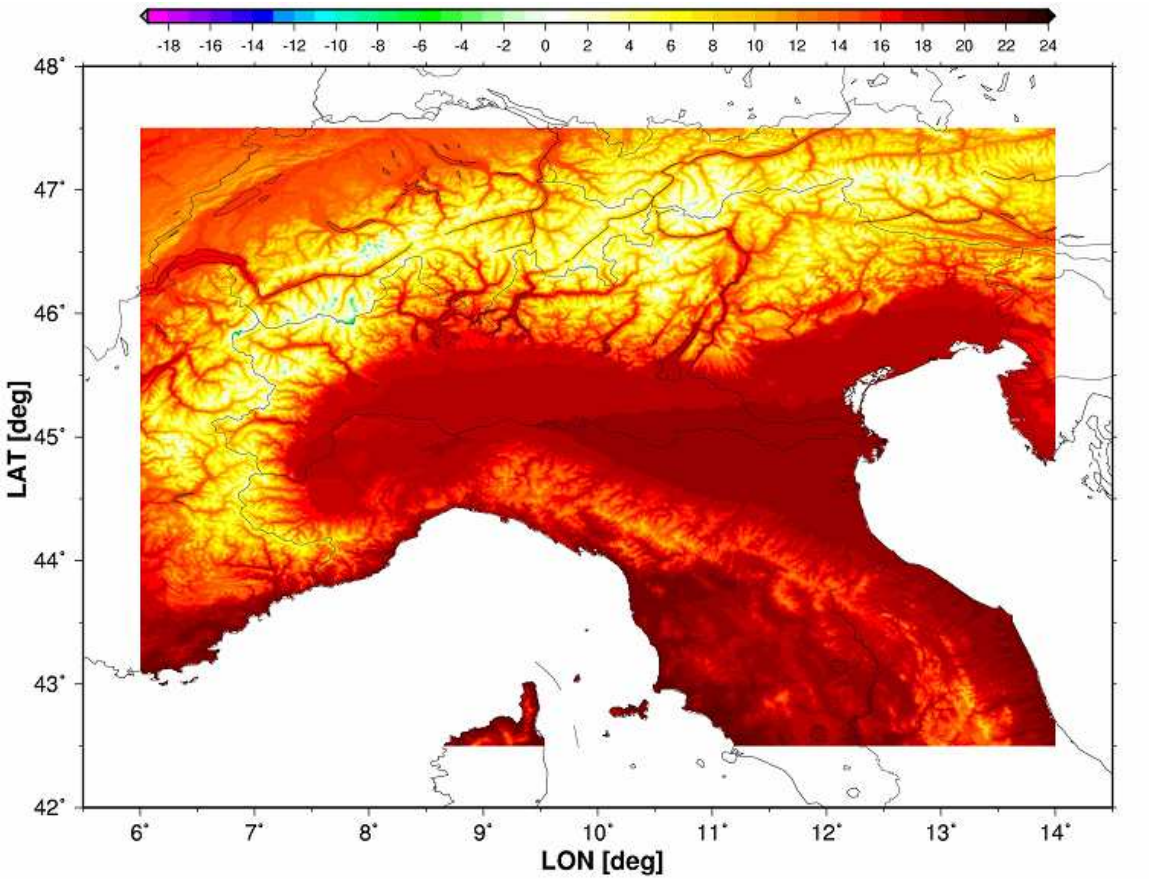

Fig. 48 : September temperature map.

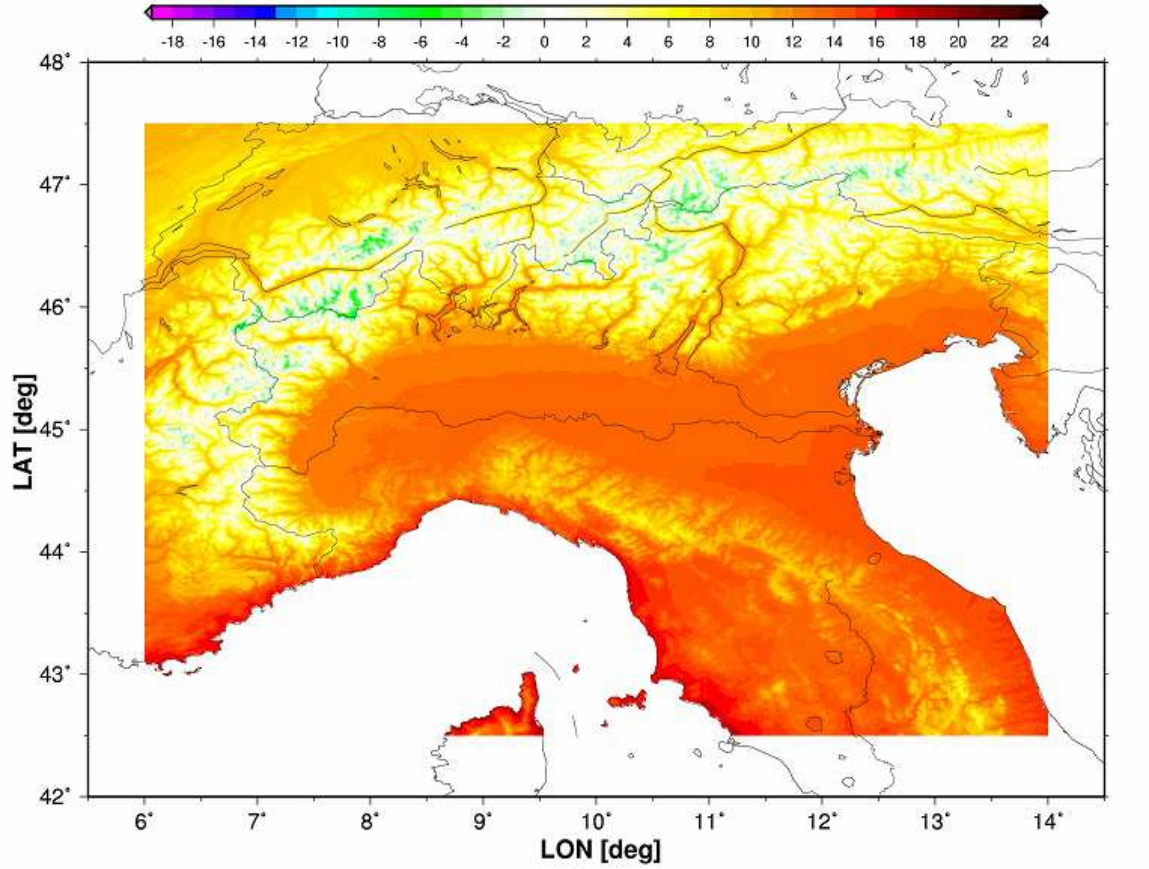

Fig.49: October temperature map

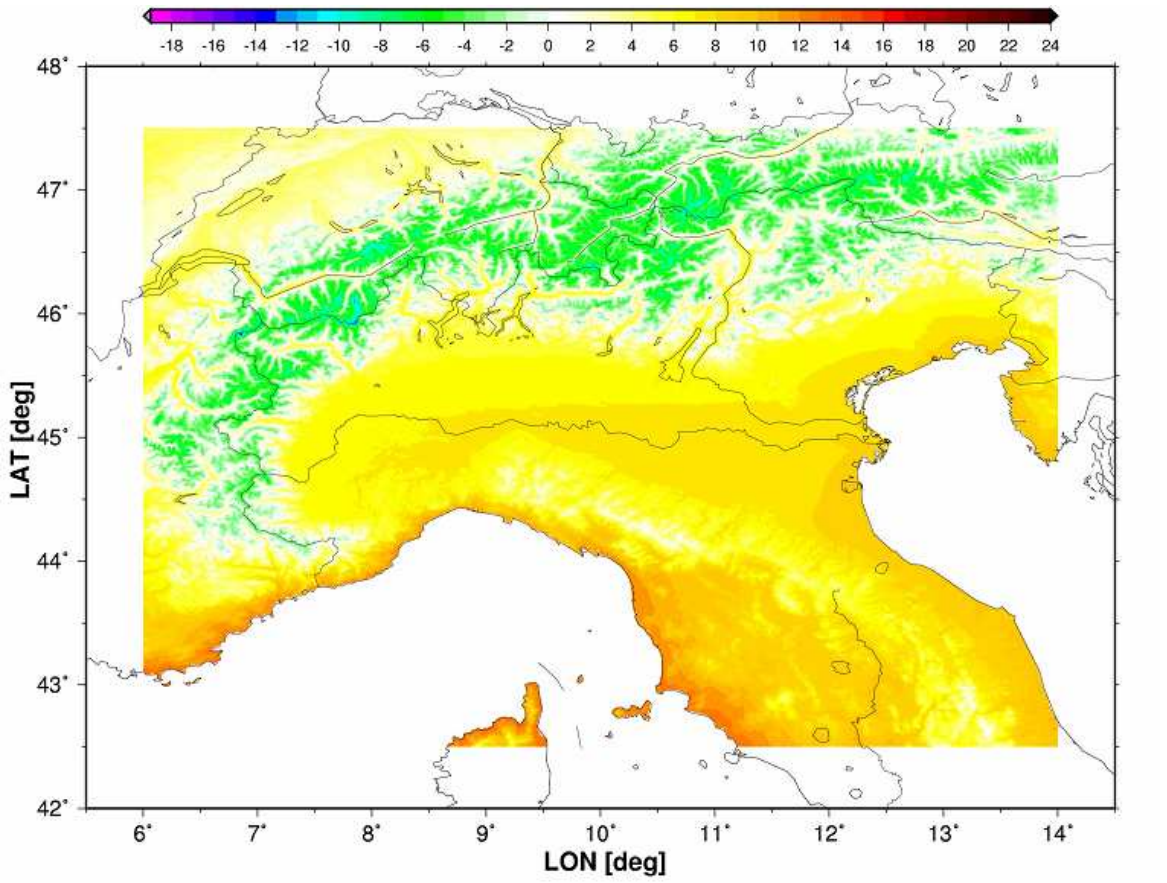

Fig. 50 : November temperature map

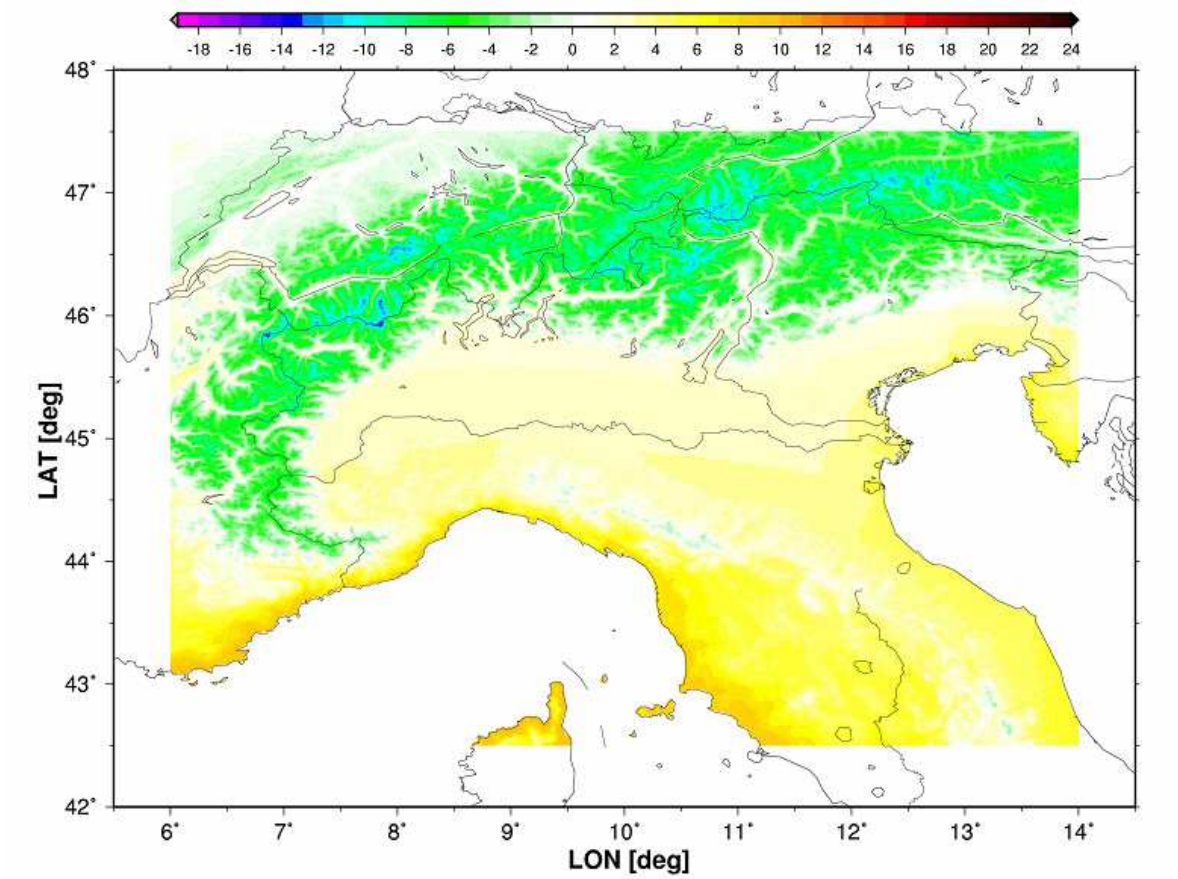

Fig. : 51 December temperature map

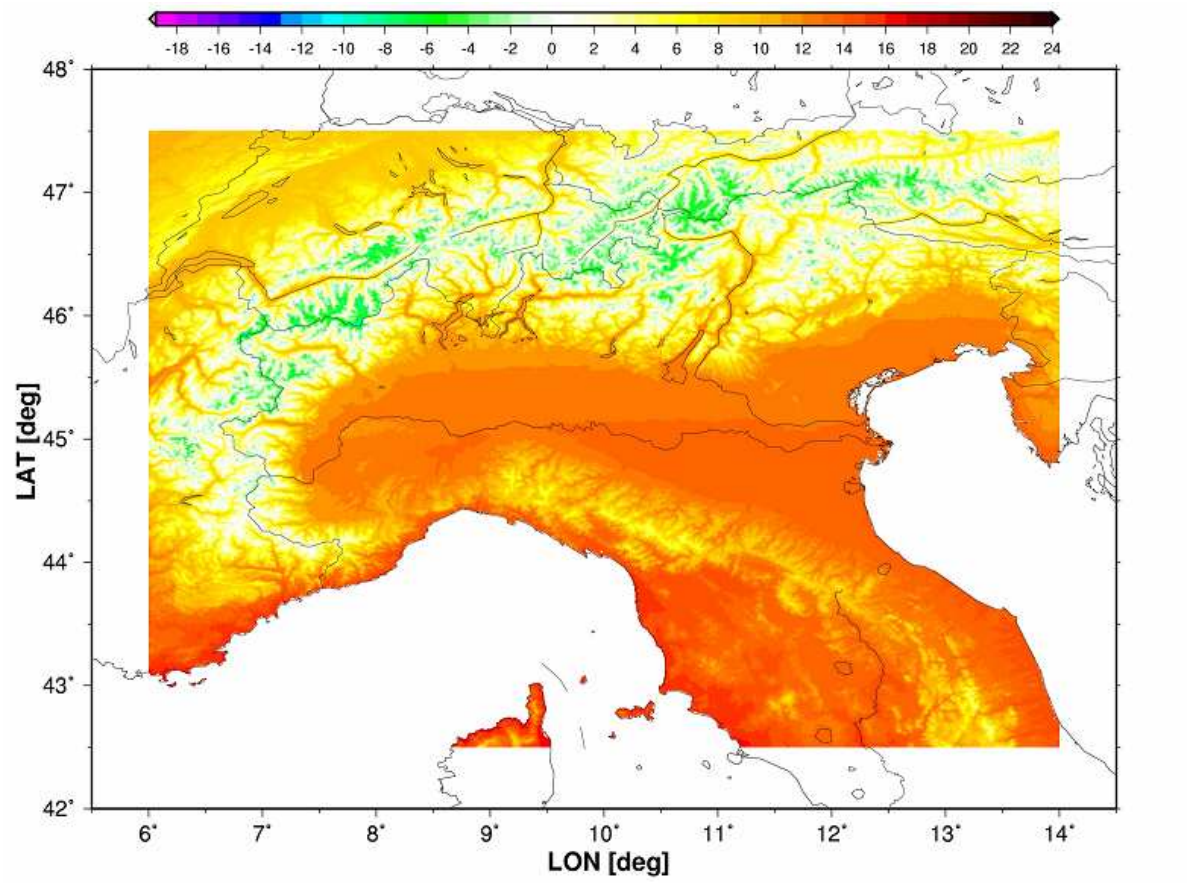

Fig. 52 : Average yearly temperature map.

References

Agnew MD, Palutikof JP. 2000. **GIS-based construction of baseline climatologies for the Mediterranean using terrain variables**. *Climate Research, 14: 115-127.*

Antonic O, Krizan J, Marki A, Bukovec D. 2001. **Spatio-temporal interpolation of climatic variables over large region of complex terrain using neural networks.** *Ecological Modelling, 138: 255-263.*

Atkinson DE, Gajewski K. 2002. **High resolution evaluation of summer surface air temperature in the Canadian arctic archipelago**. *Journal of Climate, 15: 3601-3614.*

Auer I, Böhm R, Potzmann R, Schöner W, Müller-Westermeier G, Kveton V, Cegnar T, Dolinar M, Gajic-Capka M, Zaninovic K, Maugeri M, Brunetti M, Nanni T, Carrer M, Mercalli L, Majstorovic Z, Begert M, Moisselin J-M, Ceron J-P, Bochnicek O, Zitari B, Nola P. 2005. **A High Resolution Temperature Climatology for the Greater Alpine Region (GAR)**. *ICAM Zadar, Croatia, 23rd – 27th May, 2005 Proceedings, Poster Session E04, 593-596.*

Auer I., Böhm R., Schöner W.. 2006. **EUMETNET Project ECSN/HRT-GAR: High Resolution Temperature Climatology in Complex terrain- demonstrated in the test area Greater Alpine Region (GAR).** *EMS 2006 proceedings at www.cosis.net.*

Auer I, Böhm R, Jurkovic A, Lipa W, Orlik A, Potzmann R, Schöner W, Ungersbock M, Matulla C, Briffa K, Jones P, Efthymiadis D, Brunetti M, Nanni T, Maugeri M, Mercalli L, Mestre O,

Moisselin J-M, Begert M, Müller-Westermeier G, Kveton V, Bochnicek O, Stastny P, Lapin M, Szalai S, Szentimrey T, Cegnar T, Dolinar M, Gajic-Capka M, Zaninovic K, Nieplova E. 2007. **HISTALP- historical instrumental climatological surface time series of the Greater Alpine Region.** *International Journal of Climatology, 27: 17-46.*

Benavides R, Montes F, Rubio A, Osoro K. 2007. **Geostatistical modelling of air temperature in a montainous region of northern Spain.** *Agricultural and Forest Meteorology, 146:173-188.*

Bica B, Steinacker R, Lotteraner C, Suklitsch M. 2007. **A new concept for high resolution temperature analysis over complex terrain.** *Theoretical and Applied Climatology, 90: 173-183.*

Bjornsson H. 2003. **The annual cycle of temperature in Iceland**. *Vedurstofa Islands, Report 03037.*

Böhm R. 1998. **Urban Bias in Temperature Time Series – a Case Study for the City of Vienna, Austria.** *Climatic Change, Volume 38, Number 1, January 1998 , pp. 113-128(16).*

Böhm R, Auer I, Brunetti M, Maugeri M, Nanni T, Schöner W. 2001. **Regional temperature variability in the European alps: 1760-1998 from homogenized instrumental time series.** *International Journal of Climatology, 21: 1779-1801.*

Bolstad PV, Swift L, Collins F, Regniere J. 1998. **Measured and predicted air temperature at basin to regional scales in the southern Appalachian mountains**. *Agricultural and Forest Meteorology, 91: 161-176.*

Bottyan Z, Kircsi A, Szegedi S, Unger J. 2005. **The relationship between built-up areas and the spatial development of the mean maximum urban heat island in Debrecen, Hungary.** *International Journal of Climatology, 25: 405-418.*

Brown DP, Comrie AC. 2002. **Spatial modeling of winter temperature and precipitation in Arizona and New Mexico, USA.** *Climate Research, 22: 115-128.*

Carrega P. 1995. **A method for reconstruction of mountain air temperatures with automatic cartographic applications.** *Theoretical and applied climatology, 52 (1-2): 69-84.*

Casty C, Wanner H, Luterbacher J, Esper J, Bohm R. 2005. **Temperature and precipitation variability in the european alps since 1500.** *International Journal of climatology, 25: 1855-1880.*

Champeaux J.L., Mucher C.A., Steinnocher K., Griguolo S., Wester K., Goutorbe J-P., Kressler F., Heunks C., Van Katwijk V.F.. 2000. **The PELCOM Project: a 1-km pan-European land cover database for environmental monitorino and use in meteorological models.** *Geoscience and remote sensing symposium, proceedings, IGARSS 2000, IEEE 2000 International: 1915-1917.*

Chuanyan Z, Zhongren N, Guodong C. 2005. **Methods for modelling of temporal and spatial distribution of air temperature at landscape scale in the southern Qilian mountains, China.** *Ecological modelling, 189: 209-220.*

Chung U, Choi J, Yun JI. 2004. **Urbanization effect on the observed change in mean monthly temperatures between 1951-1980 and 1971-2000 in Korea.** *Climatic Change, 66: 127-136.*

Chung .U, Yun JI. 2004. **Solar irradiance-corrected spatial interpolation of hourly temperature in complex terrain**. *Agricultural and Forest Meteorology, 126: 129-139.*

Clements CB, Whiteman CD, Horel JD. 2002. Cold-Air-Pool Structure and Evolution in a Mountain Basin: Peter Sinks, Utah. *Journal of applied meteorology, 42: 752-768.*

Collins FC, Bolstad PV., 2007, **A Comparison of Spatial Interpolation Techniques in Temperature Estimation.** *Available online at http://www.ncgia.ucsb.edu/conf/SANTA_FE_CD-ROM/sf_papers/collins_fred/collins.html.*

Colombo T, Pelino V, Vergari S, Cristofanelli P, Bonasoni P. 2007. **Study of temperature and precipitation variations in Italy based on surface instrumental observations**. *Global and Planetary Change 57: 308-318.*

Daly C, Taylor GH, Gibson WP, Parzybok T. 1998. **Development of High-Quality Datasets for the United States for the United States and beyond.** *Transactions of the ASAE, vol. 43, n°6, pp. 1957-1962.*

Daly C, Gibson WP, Taylor GH, Johnson GL, Pasteris P. 2002. **A knowledge-based approach to the statistical mapping of climate.** *Climate research, 22: 99-113.*

Daly C, Helmer EH, Quinones M. 2003. **Mapping the climate of Puerto Rico, Vieques and Culebra**. *International Journal of Climatology, 23: 1359-1381.*

Daly C. 2006. **Guidelines for assessing the suitability of spatial climate data sets.** *International Journal of Climatology, 26: 707-721.*

Daly C, Halbleib M, Smith JI, Gibson WP, Doggett MK, Taylor GH, Curtis J, Pasteris, PA. 2008. **Physiographically-sensitive mapping of temperature and precipitation across the conterminous United States.** *International Journal of Climatology*, *DOI: 10.1002/joc.1688.*

Dyras I, Dobesch H, Grueter E, Perdigao A, Tveito OE, Thornes JE, Van der Wel F, Bottai L. 2005. **The use of Geographic Information Systems in climatology and meteorology: COST 719**. *Meteorol. Appl., 12: 1-5.*

Dodson R, Marks D. 1997. **Daily air temperature interpolated at high spatial resolution over a large mountainous region**. *Climate research, 8, 1-20.*

Eliasson I, Svensson MK. 2003. **Spatial Air Temperature Variations and Urban Land Use - A statistical approach.** *Meteorol. Appl., 10: 135-149.*

Efron B, Gong G. 1983. **A leisurely look on the bootstrap, the jackknife and the cross-validation**. *The American Statistician, 37 (1): 36-48.*

Fan Y, Van den Dool H. 2008. **A global monthly land surface air temperature analysis for 1948-present.** *Journal of Geophysical Research , 113, D01103, doi:10.1029/2007JD008470.*

Gylfadottir SS. 2003. **Spatial Interpolation of Icelandic monthly mean temperature data.** *Vedurstofa Islands, Report 03006.*

Goodale CL, Aber JD, Ollinger SV. 1998. **Mapping monthly precipitation, temperature, and solar radiation for Ireland with polynomial regression and a digital elevation model**. *Climate Research, 10: 35-49.*

Hancock PA, Hutchinson MF. 2005. **Spatial Interpolation of large climate data sets using bivariate thin plate smoothing splines.** *Environmental Modelling and Software, 21: 1684-1694.*

Hartkamp AD, De Beurs K, Stein A, White JW. 1999. **Interpolation techniques for climate variables.** *NRG-GIS Series 99-01. Mexico, D.F: CIMMYT.*

Haylock MR, Hofstra N, Klein Tank AMG, Klok EJ, Jones PD, New M. 2008. **A European daily high resolution gridded dataset of surface temperature and precipitation for 1950-2006**. *Submitted to Journal of Geophysical Research.*

Hargy VT. 1997. **Objectively mapping accumulated temperature for Ireland**. *International Journal of Climatology, 17: 909-927.*

Heuvelink GBM. 1998. **Uncertainty analysis in environmental modelling under a change of spatial scale**. *Nutrient Cycling in Agroecosystems, 50: 255-264.*

Hijmans RJ, Cameron SE, Parran JL, Jones PG, Jarvis A. 2005. **Very High Resolution Interpolated Climate Surfaces for Global Land Areas.** *International Journal of Climatology, 25: 1965-1978.*

Holdaway MR. 1996. **Spatial modelling and interpolation of monthly temperature using kriging**. *Climate Research, 6: 215-225.*

Hollis D, Perry M. 2004. **Spatial Analysis of climate trends in the UK since 1961.** *EMS Annual Meeting Abstracts,1 : 00226.*

Hudson G, Wackernagel H. 1994. **Mapping temperature using kriging with external drift: Theory and an example from Scotland.** *International Journal of Climatology, 14: 77-91.*

Jarvis CH, Stuart N. 2001. **A comparison among strategies for interpolating maximum and minimum daily air temperatures. Part I: the selection of "guiding" topographic and land cover variables**. *Journal of Applied Meteorology, 40:1060-1074.*

Jarvis CH, Stuart N. 2001. **A comparison among strategies for interpolating maximum and minimum daily air temperatures. Part II: the interaction between number of guiding variables and the type of interpolation method**. *Journal of Applied Meteorology, 40: 1075-1084.*

Karl TR, Diaz HF, Kukla G. 1988. **Urbanization: its detection and effect in the United States Climate Record.** *Journal of Climate, 1: 1099-1123.*

Kim H-S, Gangopadhyay A, Rosenfeld LK, Bub FL. 2007. **Developing a high resolution climatology for the Central California coastal region.** *Continental Shelf Research 27: 2135-2161.*

Kukla G, Gavin J, Karl R. 1986. **Urban Warming.** *Journal of Climate and Applied Meteorology, 25: 1265-1270.*

Kurtzman D, Kadmon R. 1999. **Mapping of temperature variables in Israel: a comparison of different interpolation methods.** *Climate Research, 13: 33-43.*

Lanciani A, Salvati M. 2008**. Spatial interpolation of surface weather observations in Alpine Meteorological Services**. *FORALPS technical report, 2. Univ.Trento, Dip.Ing.Civ., Trento, 40pp.*

Lennon JL, Turner JRG. 1995. **Predicting the spatial distribution of Climate: Temperature in Great Britain**. *The Journal of Animal Ecology, 64 (3): 370-392.*

Li Q, Zhang H, Liu X, Huang J. 2004. **Urban Heat Island effect on annual mean temperature during the last 50 years in China.** *Theoretical and applied Climatology, 79, 165-174.*

McKenney DW, Papadopol P, Lawrence K, Campbell K, Hutchinson M. 2007. **Customized spatial climate models for Canada**. *Forestry Research Applications, technical note No. 108.*

McKenney DW, Pedlar JH, Papadopol P, Hutchinson M. 2007. **The development of 1901-2000 historical monthly climate models for Canada and the United States.** *Agricultural and forest meteorology, 138: 69-81.*

Milewska EJ, Hopkinson RF, Niitso A. 2005. **Evaluation of Geo-Referenced Grids of 1961-1990 Canadian Temperature and Precipitation Normals**. *Atmosphere Ocean, 43(1): 49-75.*

Mitchell TD, Carter TR, Jones PD, Hulme M, New M. 2004. **A comprehensive set of high-resolution grids of monthly climate for Europe and the globe: the observed record (1901-2000) and 16 scenarios (2001-2010).** *Tyndall Centre for Climate Change research, Working paper 55, July 2004.*

Mitchell TD, Jones PD. 2005. **An improved method of constructing a database of monthly climate observations and associated high-resolution grids**. *International Journal of Climatology, 25: 693-712.*

Nalder IA, Wein RW. 1998. **Spatial interpolation of climatic normals: test of a new method in the Canadian boreal forest.** *Agricultural and Forest Meteorology, 92: 211-225.*

New M, Hulme M, Jones P. 2000. **Representing twentieth-century space-time climate variability. Part II: development of 1901-96 monthly grids of terrestrial surface climate**. *Journal of Climate, 13: 2217-2238.*

New M, Lister D, Hulme M, Makin I. 2002. **A high-resolution data set of surface climate over global land areas.** *Climate research, 21: 1-25.*

Ninyerola M, Pons X, Roure M. 2000. **A methodological approach of climatological modelling of air temperature and precipitation through GIS techniques**. *International Journal of Climatology, 20: 1823-1842.*

Ninyerola M., Pons X., Roure JM.. 2007. **Objective air temperature mapping for the Iberian Peninsula using spatial interpolation and GIS.** *International Journal of Climatology, 27: 1231-1242.*

Ollinger SV, Aber JD, Anthony Federer C, Lovett GM, Ellis JM. 1995. **Modeling physical and chemical climate of the Northeastern United States for a Geographic Information System**. *US Dep. of Agriculture, Forest Service, N-E Forest Exp. Station, General Technical Report NE-191.*

Oke, TR. 1973. **City size and the urban heat island**. *Atmospheric Environment, 7, 769-779.*

Oke, TR. 1982. **The energetic basis of the urban heat island.** *Quarterly Journal of the Royal Meteorological Society 108: 1–24.*

Pan Y, He C, Zhang Q, Chen J. 2004. **Smart distance and DEM-informed interpolation of surface air temperature of climatology in China.** *IEEE 2004, 0-7803-8742-2/04.*

Percec Tadic M, Pandzic K. 2002. **Combined use of multiple linear regression, optimal interpolation and GIS in producing temperature maps**. *EGS XXVII General Assembly, Nice, 21-26 April 2002, abstract #5938.*

Peterson TC. 2003. **Assesment of Urban versus Rural in situ Surface Temperatures in the contiguous United States: No difference found**. *Journal of Climate, 16: no.18, 2941-2959.*

Pielke RA, Mehring P. 1977. **Use of Mesoscale Climatology in Montainous Terrain to Improve the Spatial Representation of Mean Monthly Temperature**. *Monthly weather review, 105 : 108-112.*

Pons X. 1996. **Estimacion de la Radiacion Solar a partir de modelos digitales de elevaciones. Propuesta metodologica.** *VII Coloquio de Geografia Cuantitativa, GIS y Teledeteccion. Juaristi J, Moro I (eds) Vitoria-Gasteiz.*

Price DT, McKenney DW, Nalder IA, Hutchinson MF, Kestevon JL. 2000. **A comparison of two statistical methods for spatial interpolation of Canadian monthly mean climate data**. *Agricultural and Forest Meteorology, 101: 81-94.*

Robeson SM. 1994. **Influence of spatial sampling and interpolation on estimates of air temperature change**. *Climate Research, 4: 119-126.*

Satanda J. 1999. **Ground surface temperature as a function of slope angle and slope orientation and its effect on the subsurface temperature field.** *Tectonophysics, 306: 367-375.*

Skirvin SM, Marsh SE, McClaran MP, Meko DM. **Climate spatial variability and data resolution in a semi-arid watershed, south-eastern Arizona.** *Journal of Arid Environments, 54: 667-686.*

Shudo H, Sugiyama J, Yokoo N, Oka T. 1997. **A study on temperature distribution influenced by various land uses**. *Energy and buildings, 26: 199-205.*

Steinacker R. 2005. **Climatological Evaluation of the temperature of lowlands and valleys in the alpine region.** *A publication VERACLIM- MAS with VERA, ZAMG Vienna.*

Tveito OE, Førland EJ. 1999. **Mapping temperatures in Norway applying terrain information, geostatistics and GIS.** *Norwegian Journal of Geography, Volume 53, Number 4, 31 December 1999 , pp. 202-212(11).*

Tveito OE, Forland EJ, Alexandersson H, Drebs A. 2001. **Nordic Climate Maps**. *NordKlim, Norwegian meteorological institute, report no. 06/01.*

Tveito OE. 2002. **Spatial distribution of winter temperature in Norway related to topography and large-scale atmospheric circulation.** *IAHS PUB kick-off Workshop, Brasilia, Brazil, 20-22 November 2002*.

Tveito OE, Bjordal I, Skjevalg AO, Aune B. 2005. **A GIS-based agro-ecological decision system based on gridded climatology.** *Meteorol. Appl. 12, 57-68.*

Ustrnul Z, Czekierda D. 2003. **Climatological air temperature maps for Poland as the GIS applications results.** *Geophysical Research Abstracts, 5: 07283.*

Ustrnul Z, Czekierda D. 2005. **Application of GIS for the development of climatological air temperature maps: an example from Poland**. *Meteorol. Appl. 12, 43-50.*

Vicente-Serrano SM, Saz-Sanchez MA, Cuadrat JM. 2003. **Comparative analysis of interpolation methods in the middle Ebro Valley (Spain): application to annual precipitation and temperature.** *Climate research, 24: 161-180.*

Willmott CJ, Matsuura K. 1995. **Smart interpolation of annually averaged air temperature in the United States**. *Journal of applied Meteorology, 34: 2577-2586.*

Willmott, CJ, Matsuura, K. 2006. **On the use of dimensioned measures of error to evaluate the performance of spatial interpolators.** *Journal of Geographical Information Science, Volume 20, Number 1.*